Number 1 Issue 1 October 2011

International Biotechnology Color Journal

A Scientific Peer Reviewed Journal with Focus on BIOTECHNOLOGY
and Covering Its Many Hues, Tints, Tones & Shades

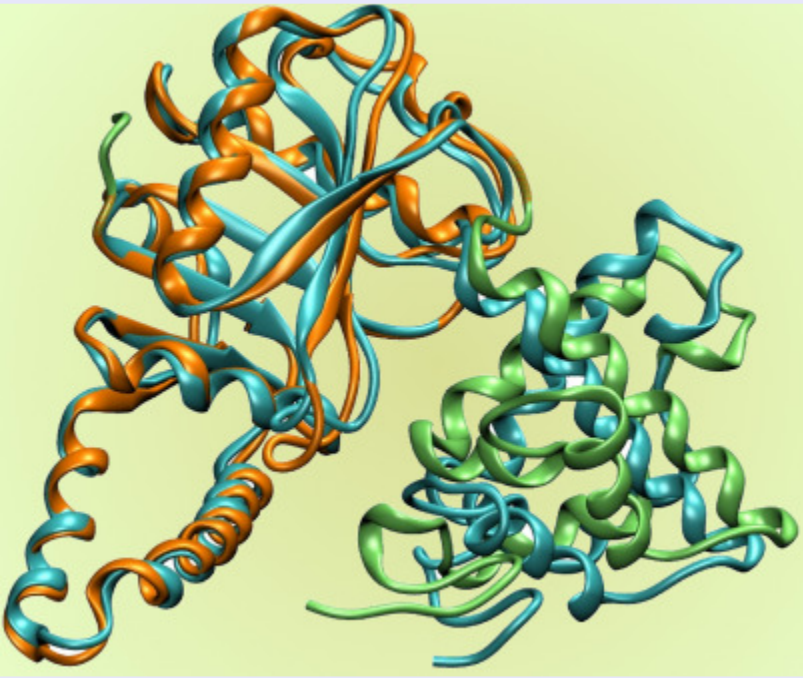

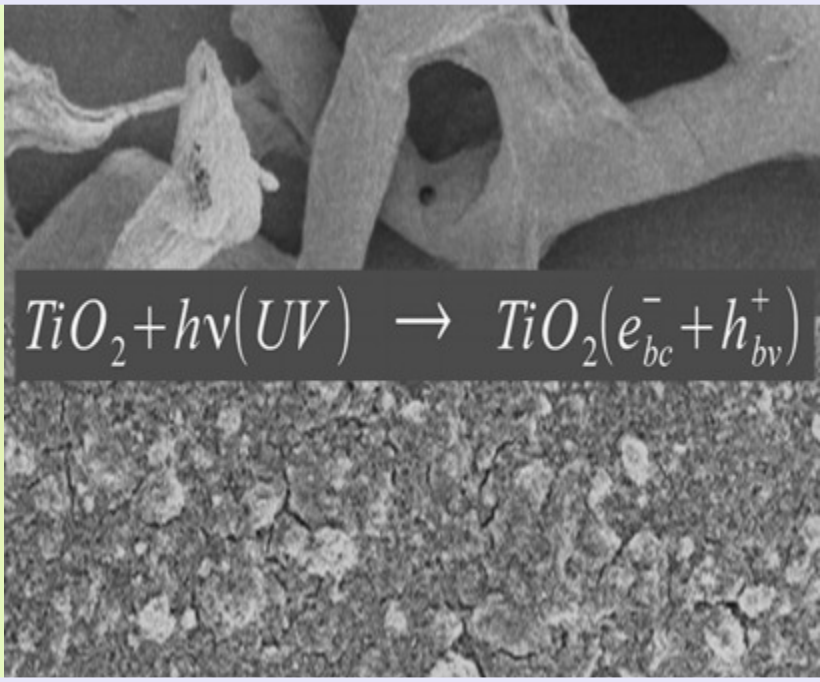

Non-conventional biological discoloration system
Physiological effects of quality protein maize products
Guide to protein homology modeling

Produced and hosted by *Centro de Investigación Científica de Yucatán, A.C.*,
in collaboration with *Universidad Nacional Autónoma de México*,
and the *International Foundation for Biotechnology Research & Early Stimulation in the Culture of Health, Nutrition, Sport, Art, Science, Technology & Society*

Number 1 Issue 1 October 2011

full text provided by www.ibcj.org.mx

International Biotechnology Color Journal

A Scientific Peer Reviewed Journal with Focus on BIOTECHNOLOGY and Covering Its Many Hues, Tints, Tones & Shades

WELCOME

We are delighted to publish this, the starting issue of the **INTERNATIONAL BIOTECHNOLOGY COLOR JOURNAL** (IBCJ).

The present publication has been produced with a considerable effort from many people, but amongst all, we are in debt to Dr. Susana Lozano Muñiz for the original idea, and the organization of the initial meetings. A brief historical account of the events leading to this Journal is included as the first article within the present issue.

The Scope of the Journal intends to cover all aspects of Biotechnology, from the science behind it, to the social impact of its use. The Journal was conceived as a COLOR periodical, where the colors are associated with the various topics within the scope of this journal. Thus, each paper is tagged with the Color assigned to the topic best representing its content and aim, according to its authors. At least for now, it is not the intention of the Editorial Board to cover all topics on every issue, therefore, the so called sections, are not sections in the classical sense, but more a guide to the reader, who may use the color to quickly select those papers with contents closer to his personal interests.

Currently, the Chief Editor of the IBCJ is Dr. José Juan Zúñiga Aguilar and the present list of editors by color is given in the Journal's Home Page. If you wish to submit a contribution please send it to the chief editor with a suggestion of the best matching COLOR (topic).

The members of the editorial board have made an effort to peer-review every contribution, regardless of who the authors are. That will apply to the papers submitted by the editorial Board. When this is the case, the editor in charge of handling the paper is never the same submitting the paper. It is my personal view that science should be taken seriously, if the scientific publications derived from it are meant to have an impact. Therefore, we shall make no exception to this rule.

In addition, we are making an effort to reduce prejudicial or biased personal opinions to interfere with the peer-review process. Therefore, every editor is asked to carefully consider the reviewers' criticisms and comments. Then he(she) should ask the reviewer to filter out any comments of a personal nature that may marred the scientific grounds of the criticism itself. In addition, before a submitted draft is turned down, we carefully consider if the reviewers have found enough positive aspects in the contribution, and if so, the editor in charge may give the authors an opportunity to rewrite and resubmit the paper.

We are also considering the implementation of a blind peer-review, to reduce, as much as possible, the bias in the process.

We hope the contents of the IBCJ are of interest to you. Please feed us back with your comments and suggestions.

Yours Sincerely,
Rogelio Rodríguez-Sotres
Journal's Director.

Number 1 Issue 1 October 2011

full text provided by www.ibcj.org.mx

International Biotechnology Color Journal

A Scientific Peer Reviewed Journal with Focus on BIOTECHNOLOGY and Covering Its Many Hues, Tints, Tones & Shades

Table of Contents

Number 1 Issue 1 October 2011

full text provided by www.ibcj.org.mx

International Biotechnology Color Journal

A Scientific Peer Reviewed Journal with Focus on BIOTECHNOLOGY and Covering Its Many Hues, Tints, Tones & Shades

INTERNATIONAL BIOTECHNOLOGY COLOR JOURNAL

EDITORIAL SECTION

International Biotechnology Color Journal (IBCJ) is an electronic Open Access journal, devoted to rapidly publishing full peer-reviewed articles covering all the fields of biotechnology. Though the central focus of IBCJ is to publish scientific papers, it will provide a forum for reviews of special interest, notes presenting relevant findings in a short format, essays with new technical advances or the substantial modification of reported protocols, book reviews, scientific meetings, and letters to the editor. Instructions for every type of contribution are presented in the journal's Homepage and also in PDF format.

Initially, IBCJ will have three editions a year, appearing in February, June and October. It is the journal interest to speed up the reviewing process to allow the publication of accepted contributions in the next edition of the journal. On its opening edition, we presented the first number in November, 2011, with two full articles, a scientific review, and a book review.

The Editorial Board of IBCJ is fully committed to publish articles that contribute to the innovation of all areas of biotechnology. Contributions are reviewed from a rigorous optic of scientific criticism; thus, any original contribution that fits within the scope of the journal, particularly those that promote the advancement of biotechnology are particularly welcome.

José Juan Zúñiga-Aguilar
Chief Editor.

Editorial comments to the contents in issue 1

by José Juan Zúñiga-Aguilar

In the first contribution, Henao-Jaramillo et al., present the comparison of two methods for the discoloration of Reactive Black 5, a broadly-used dye present in waste effluents of textile industries. The photocatalysis with TiO2, and the combination of Trametes versicolor followed by photocatalysis effectively remove the dye from effluents; however, the use of Hydra attenuata as biosensor demonstrate that photocatalysis alone provides a better decontamination method, as it reduces the toxicity of the product. This procedure represents a good environmental-safe option for the treatment of the industrial waste effluents.

In a paper related to the production of nutrimental supplements, Robles-Ramírez et al., present the evaluation of the effects of nixtamalization and extrusion process over the protein quality and fiber content of quality protein maize (QPM), compared to a commercial brand product. From their findings, extrusion of QPM constitutes a better alternative to commercial products, but nixtamalization did not produce a difference in the nutrimental properties of QPM. The quality of protein and fiber content provided by extrusion of QPM improved beneficial effects to healthin comparison to those provided by commercial products.

In the third contribution, Chavelas-Adame et al. report the comparison of non-commercial methods to the homology modeling of the 3D structure of proteins, with emphasis in a new developed protocol, the Rd.HHM score, which in combination with other quality measures allows the best identification of 3D models with a biological relevant folding pattern. This review offers a detailed comparison of models obtained with freely available software and open-access internet services. These models are useful tools to better correlate the amino acid sequence and the 3D structure of proteins with their biological functions.

Number 1 Issue 1 October 2011

full text provided by www.ibcj.org.mx

International Biotechnology Color Journal

A Scientific Peer Reviewed Journal with Focus on BIOTECHNOLOGY
and Covering Its Many Hues, Tints, Tones & Shades

Brief History of the foundation of the INTERNATIONAL BIOTECHNOLOGY COLOR JOURNAL

The **International Biotechnology Color Journal** (IBCJ) is the official quarterly publication of the **International Foundation for Biotechnology Research & Early Stimulation in the Culture of Health, Nutrition, Sport, Art, Science, Technology & Society A.C.** (IFBR&ESCHNSAST&S).

The IFBR&ESCHNSAST&S was initiated as an organization aimed to bring together the needs of the Society for more efficient solutions to our many problems, with the need for environmentally friendly and sustainable solutions. Biotechnology can be a powerful tool to such aim, but before it can be widely applied, two things are needed. On one hand, extensive research is needed to render the knowledge-based technical solutions. The sustainability, the possible environmental and health effects of the applications derived from those studies would have to be assessed, and research is also needed there. On the other hand, Society as a whole will have to be more aware of these technological developments, because with every new technology, new horizons open, but also a need arises for qualified individuals, who must handle the technical details of its use. In addition, the final user must be aware of the precautions to be taken, in order to minimize risk.

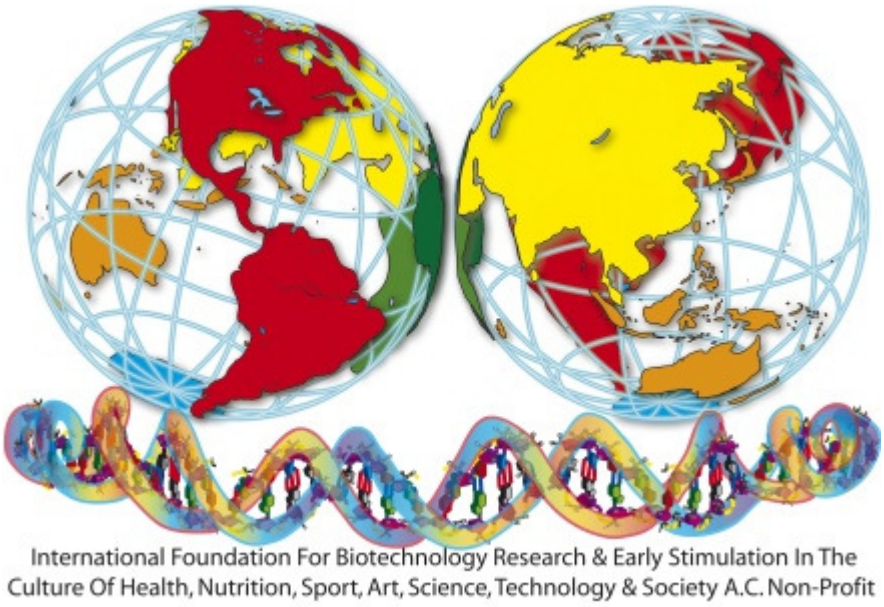

Figure 1. Registered logo of the International Foundation for Biotechnology Research & Early Stimulation in the Culture of Health, Nutrition, Sport, Art, Science, Technology & Society A.C. (with the foundation's permission).

With the support of many members of the national and international scientific community, we had the honor to sign the constitutive act of the foundation in the Heroic City of Huajuapan de León, Oaxaca, on September 14th, 2009, at the NOTARÍA PÚBLICA No. 61 de los ESTADOS UNIDOS MEXICANOS. As a civil association and nonprofit organization. Its logo was duly registered and is shown in figure 1.

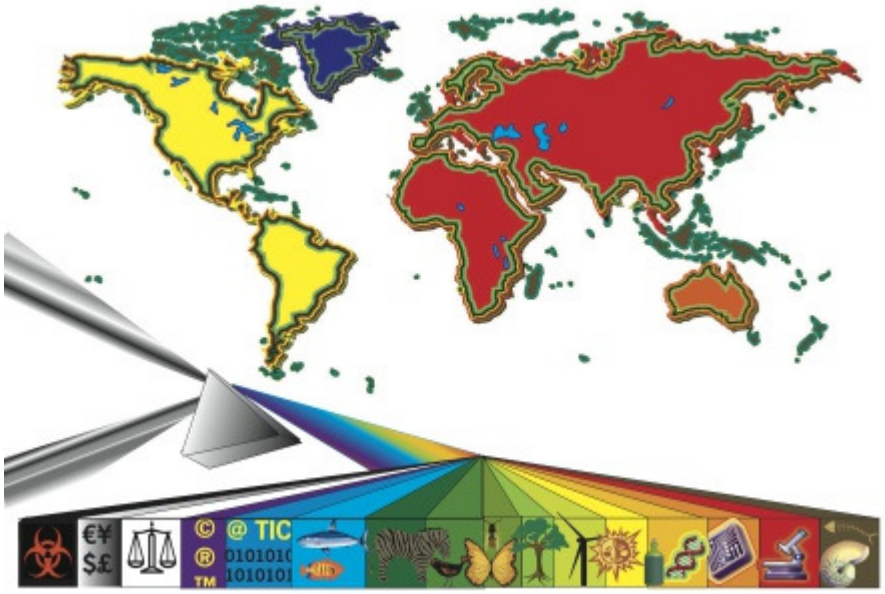

Figure 2. Registered logo of the INTERNATIONAL BIOTECHNOLOGY COLOR JOURNAL (all rights reserved).

The main goals of the foundation are:

1. To promote sustainable human development based on a high academic preparedness, and integrative learning through early stimulation in the culture of health, nutrition, sports, arts, science, technology and society. The target population are children and young people from urban, rural and indigenous communities, who should broaden their horizons, and grow, both, personally and professionally.

2. To promote and strengthen the scientific research as a means to the expansion of the limits of knowledge, and to the preparation of skilled and qualified human resources, by granting scholarships, creating and strengthening groups, networks or academic bodies, acquiring or strengthening infrastructure for education biotechnological and scientific research. These activities should raise life quality and welfare of individuals and society.

3. Support popular science and biotechnology so that society in general may raise its scientific and technological culture and learn of appreciate its benefits and assess the risks. A better understanding of science and technology should also be promoted through better academic curricula, teaching material, and the continuous education of teachers and educational authorities. A higher level of education may bring fairness and equality of opportunities to society.

4. Promote the collective knowledge through scientific events and instruments to broadcast scientific, educational and biotechnological information, such as the **IBCJ**.

Although all of the above goals are considered equally important, the latter one received the strongest support from the scientific community. And especially from the Yucatan Center for Scientific Research (CICY), the academic and scientific institution hosting the **IBCJ** website (www.ibcj.org.mx).

The **IBCJ** started as an idea a couple of years ago, and I sent invitations to all the scientists who has previously shown some interest in the journal. There, we made a list of all those interested in taking an active roll in the creation of the journal. Later, periodical meeting were adjourned and in those meeting the ideas did solidify. Thanks to the very generous resource management of Dr. Jose Juan Zúñiga made the **Centro de Investigación Científica de Yucatán A.C.** (CICY) to provide web page hosting facilities, along with the support of their computer experts. This paved the way to the actual production of the first issue.

Essential work is performed by the journal's manager, Dr. Rogelio Rodriguez Sotres, a researcher at the Universidad Nacional Autónoma de México (UNAM). He has done a great job to make the publication of this journal possible, because he is an enthusiastic and spares no effort to carry out this assignment, so we are grateful for the support he has provided us.

At the same time, several colleagues sent their manuscripts to be reviewed, even though they knew the journal was still work in progress. At the time, my experience as a Journal Editor and as a Journal Manager was limited so I appointed other collaborators to help me with the task. Out of the manuscript submitted 3 were sent back for revision, and the revised version was considered acceptable by the reviewers. Those are the ones included in this, our first issue, and we consider them to be of high quality.

Though too many to be listed here, I thank to all who have given support the foundation and the Journal.

Best regards,

Susana Lozano Muñiz

President of the Foundation

Number 1 Issue 1 October 2011

full text provided by www.ibcj.org.mx

International Biotechnology Color Journal

A Scientific Peer Reviewed Journal with Focus on BIOTECHNOLOGY and Covering Its Many Hues, Tints, Tones & Shades

Important announcement

The **International Foundation for Biotechnology Research & Early Stimulation in the Culture of Health, Nutrition, Sport, Art, Science, Technology & Society A.C.** is currently organizing the **Biotechnology Summit 2012** in collaboration with International Centre for Genetic Engineering and Biotechnology (ICGEB), American Society for Microbiology (ASM), Sociedad Mexicana de Biotecnología y Bioingeniería (SMBB) Yucatán delegation, Centro de Investigaciones y Estudios Avanzados del IPN (CINVESTAV-IPN), Universidad Autónoma Metropolitana Unidad Cuajimalpa (UAM-C), Universidad Autónoma de Nuevo León, Facultad de ciencias Biológicas (UANL FCB), Secretaría de Educación Pública (SEP), Consejo Nacional de Ciencia y Tecnología (CONACYT), Universidad Nacional Autónoma de México (UNAM), among others.

The **Biotechnology Summit** will be held in Merida, Yucatan, on March 12 to 21, 2012.

More information is available at the following link:

http://www.icgeb.org/meetings-2012.html

The program is available at the following link:

http://community.asm.org/events/biotechnologysummit2012meridayucatanmexico/

http://www.researchgate.net/conference/Biotechnology_Summit_2012_March_12-21_2012/sessions/

And soon at http://www.bio.edu.mx/

International Biotechnology Color Journal

Use of a non-conventional biological system and advanced oxidation process with TiO_2/UV to the discoloration of reactive black 5.

Lina María Henao-Jaramillo[1], *Jorge Andrés Fernández-González*[1], *Balkys Esmeralda Quevedo-Hidalgo*[1], *Alex Enrique Florido-Cuellar*[2], and *Aura Marina Pedroza-Rodríguez*[1*].

[1] Grupo de Biotecnología Ambiental e Industrial (GBAI). Departamento de Microbiología. Facultad de Ciencias Básicas. Universidad Javeriana.

[2] Grupo de Materiales Semiconductores y Superiónicos. Departamento de Física. Facultad de Ciencias. Universidad del Tolima. Alto de Santa de Helena.

*To whom all correspondence should be sent.

Chief Editor: José J. Zúñiga-Aguilar. Area Editor: Susana Lozano. Recieved: June 8, 2010. Revised version: September 20, 2011. Accepted: October 30,2011.

Abstract

Trametes versicolor and homogeneous photocatalysis with TiO_2 were used for the removal of 300 mg l^{-1} of Reactive Black 5 (RB5). A biological pre-treatment in bubble column was set up with 525 ml of non-sterilized basal medium inoculated with *T. versicolor* immobilized in *Luffa cylindrica* sponge for 7 d at 25ºC. After 4 d of culture, 98% of color removal (CR) was reached with laccase activity of 8 U l^{-1} and pH 4.5. The pre-treated dye was exposed to a photocatalytic treatment in quartz reactor (sequential) with its controls. Within a period of 12 h 98% of reduction, 7% (photolysis) and 2% in absence of light was reached. Photocatalisys was used to remove 300 mg l^{-1} of RB5 without biological pre-treatment. RB5 solutions rapidly decolorized reaching values of 99% (299 mg l^{-1}) in 12 h of irradiation. The dye's toxicological effect was determined using *Hydra attenuata*. At 300 mg l^{-1} and the dye treated only by photocatalysis did not present any toxicological effect. The effluent pre-treated with *T. versicolor* lead to 50% of mortality on *H. attenuata* to 5.25 mg l^{-1}. The effluent post-treated with TiO_2 also had the same lethality of 50% at a concentration of 1.6 mg l^{-1}.

***Contact address:** Grupo de Biotecnología Ambiental e Industrial (GBAI). Departamento de Microbiología. Facultad de Ciencias. Universidad Javeriana. Carrera 7 No 48-32, Bogotá, Colombia. e-mail: apedroza@javeriana.edu.co

Abbreviations: RB5, Reactive Black Five; *T. versicolor*, *Trametes versicolor; P. ostreatus*, *Pleurotus ostreatus*; *P. chrysosoporium*, *Phanerochaete chrysosporium*; LCS, *Luffa cylindrica* sponge; *H. attenuata*, *Hydra attenuata*; LiP, Lignin Peroxidase; MnP, Manganese Peroxidase ; EWB, Extract Wheat Bran.

Keywords: *Trametes versicolor*, homogeneous photocatalysis with TiO_2 and reactive black 5

Introduction

The reactive black 5 (RB5: $C_{26}H_{21}N_5O_{19}S_6Na_4$) is a diazo dye composed of an auxochrome-chromophore complex, consisting of 2 azo groups and 4r aromatic rings. The molecule also has sodium sulphate ions (Na^+SO_3) that provide it water solubility. This dye is widely used for dying cotton fibers within the textile industry. However, the dye is not completely adhered to the material. As a result, approximately 50% is released as wastewater into aquatic systems (1,2). This fact generates severe environmental impacts affecting the aesthetic value of water bodies (3), diminishing the dissolved oxygen concentrations causing the subsequent death of organisms in different trophic levels (4). Finally, when the dye is biotransformed under certain natural conditions, new intermediaries, which are often more toxic than the pattern compound may be produced (5).

Azo dyes are designed to endure tough conditions like being in contact with sweat, soap, water, light and oxidizing agents; this makes them very stable compounds and less susceptible to biodegradation (6). Therefore, the biological degradation by conventional treatment is related with microbial biomass absorption. Yet, there is not a complete mineralization (7). White-rot fungus such as *Trametes versicolor,* are capable of oxidizing a broad variety of dyes like azo, triphenylmethane, polymers, and heterocyclic phthalocyanines (8). The removal is carried out by the combined action of two processes. The first one is physical and it is associated with adsorption phenomena. The second one is a biochemical reaction dealt by a group of nonspecific enzymes, such as lignin peroxidase (LiP), manganese peroxidase (MnP) and laccase. These enzymes catalyze the oxidation of recalcitrant substances, through the removal of electrons forming unstable cationic intermediates that can be mineralized to CO_2 and H_2O (9-11). Currently, Non-conventional biological treatments with white rot fungi have been used as a bio-technological alternative, especially when the fungal biomass is immobilized on inert and non-inert supports (10). Nevertheless, these treatments can lead to none complete bio transformations which implies changes in the color range without a total discoloration. On top of that, fungi as a biological system are susceptible to certain environmental conditions. They need longer time processes and depending on the toxicity of the pollutant, they can also be inhibited. This situation narrows their use or implies the necessity of performing a complementary treatment (12).

One possibility is the use of advanced oxidation processes such as photocatalysis with TiO_2. The photocatalytic process for the removal of dyes such as RB5 begins with the production of reactive pair h^+/e^- in the valence band and the conduction band. These species are generated by the incidence of high energy light source (Eg 3.2 eV) on the TiO_2 (equation 1)

$$TiO_2 + h\nu(UV) \rightarrow TiO_2(e^-_{bc} + h^+_{bv})$$

Equation 1

The electron promoted and the photo-generated hole can participate in redox reactions with various chemical species such as water, hydroxide ion (OH^-), organic compounds and oxygen. Thus, the photocatalytic process includes oxidative and reductive stages. In the oxidative phase, photogenerated holes can directly oxidize the dye adsorbed to the semiconductor surface, according to the equation 2.

$$RB5_{ads} + h^+_{bv} \rightarrow 26\, RB5^{\bullet +}_{oxidized}$$

Equation 2

Furthermore, the photogenerated holes can also oxidize H_2O surrounded creating hydroxyl radicals, which can then diffuse to the aqueous medium and oxidize the azo dye, generating hydroxylated intermediates. This, by successive reactions, would evolve to the final products of the mineralization (equations 3, 4).

$$H_2O + TiO_2(h^+_{bv}) \rightarrow OH^{\bullet} + H^+ + TiO_2$$

Equation 3

$$BR5_{ads} + OH^{\bullet} \rightarrow RB5^{\bullet +}_{oxidized} \rightarrow products + CO_2 + H_2O$$

Equation 4

In the reductive stage, other species can be formed that would induce the degradation of the dye in a complementary manner. It is known that photogenerated electrons are transferred to a primary acceptor like oxygen (O_2), such reduction leads to the formation of superoxide anion radical ($O^{\bullet -}_{2(ads)}$), which then continue the reduction until peroxide dianion ($O^{2-}_{2(ads)}$) is formed. Alternatively, a sequence of protonation-reduction-protonation generates hydrogen peroxide (H_2O_2), which may contribute to the degradation of the dye, either acting as a direct electron acceptor or as an indirect source of hydroxyl radicals (equations 5, 6).

$$O_2 + e^-_{bc} \rightarrow O_2^{\bullet -} \quad \text{(superoxide dianion)}$$

Equation 5

$$O_2^{\bullet -} + e^-_{bc} \rightarrow O_2^{2\bullet -} \quad \text{(peroxide dianion)}$$

Equation 6

The dye's transformation is favored by the velocity of the redox reactions. The use of photocatalysis as a combined treatment to the biological system would provide a color removal close to 100%, considering the fact that the chromophore group would be completely modified (12).

The objective of this work was to investigate the efficiency of the treatment of BR5 dye with two processes, i.e., biological pre-treatment with *T. versicolor* immobilized on *Luffa cylindrica* sponge (LCS) followed by homogeneous photocatalysis using TiO_2 and photocalysis as a single treatment.

Material and Methods

Microorganisms and production of the immobilized biomass on Luffa cilyndrica sponge

T. versicolor was cultured in an extract wheat bran agar (EWB) at 30 ºC for 8 d (13). The LCS was cut into pieces of 5 mm x 5 mm and washed with distilled water. These cubes were sterilized by autoclave at 121 ºC, at 15 for 15 min. Ninety sterilized cubes were deposited into aluminum box containing 150 ml of EWB agar and fifteen agar plugs from the leading edge which were used as inoculum. The culture was incubated at 30 ºC, for 8 d.

Biological removal in bubble column reactor and operational conditions

The basal medium used to evaluated the biological discoloration contained: D-glucose 2 g l-1, KH2PO4 2 g l^{-1}, NH_4Cl 0.050 g l^{-1}, $MgSO_4 \cdot 7H_2O$ 0.5 g l^{-1}, $CaCl_2 \cdot 2H_2O$ 0.1 g l^{-1}, thiamine 100 mg l^{-1}, RB5 300 mg l^{-1} and 10 ml of the trace element solutions ($MnSO_4$ 0.5 g l^{-1}, $FeSO_4 \cdot 7H^2O$ 0.1 g l^{-1}, $ZnSO_4 \cdot 7H_2O$ 0.1 g l^{-1}) pH 4.5 (14). The biological treatment was performed in reactors made up of glass tubing (5 cm inner diameter, 50 cm long) packed with 67 mg mg^{-1} of biomass immobilized on LCS and 525 ml of non-sterilized basal medium with RB5. The reactors were maintained at 25 oC, with an air flow rate of 1 l min^{-1}. The process was evaluated for 7 days. The values in the figures correspond to the mean values of two replicates with a standard deviation of less than 15%. A control test, the adsorption to the single support (LCS) was evaluated under the same conditions of the biologic treatment. The effluent treated by *T. versicolor* was stored under refrigeration at 4ºC until further use in the photocatalytic reactor. The parameters evaluated in this kinetics were color removal or discoloration (%), glucose concentration (15), the enzymatic activity laccase (16), MnP activity (17), LiP activity (18) and pH. The immobilized biomass was observed by scanning electron microscopy.

Photocatalytic removal with TiO_2 to sequential treatment and photocatalytic treatment without biological treatment

- Selection of the wavelength and TiO_2 concentration

In this study 22 experimental designs were used in order to select the wavelength (nm) and the TiO2 concentration. This design was applied using Design Expert 6.0® and Statistical® with two factors at two levels. Two different concentrations of TiO_2 (0.5% and 1% w/v) and two wavelength (254 nm and 366 nm) were chosen as the critical variables. The response variable was color removal (%).

For the photocatalytic testing, a sample (1 ml of effluent pre treatment in biological reactor) was poured in a quartz cuvette with different TiO2 concentrations (table 1). The suspensions were magnetically stirred in the absence of light for 30 min to attain adsorption-desorption equilibrium between dye and TiO2. The samples were illuminated with a deuterium lamp of 30 W, changing the wavelength according to the design. The samples were taken after 20 min of irradiation; the TiO_2 was separated by centrifugation at 6000 rpm for 15 min. The residual color was measured at 597 nm using a spectrophotometer Genesis 21 and the absorbance was transformed in dye concentration using the standard curve (0.1-20 mg l^{-1}).

- Kinetics in photocatalytic reactor

The best concentration of TiO_2 and the wavelength were used to evaluate the photocatalytic activity in reactor using two treatments: (T1) sequential treatment (biological pre-treatment/photocatalytic pos-treatment) and (T2) photocatalytic treatment without prior biological treatment (300 mg l^{-1}). These experiments were carried out in a quartz photoreactor of 200 ml of capacity, the light source was a two 15 W high pressure mercury-vapor fluorescent lamps emission at 254 nm. It was placed parallel to the glass quartz with a distance of 5 cm between the glass and the lamp. The treatments and their controls were agitated at 120 rpm for 30 min in lack of light using a magnetic shaking previously to UV irradiation; the agitation was maintained in the same conditions during the kinetics. All the kinetics were evaluated for 14 h taking the samples every 60 min. The controls were photolysis (UV) and the adsorption (TiO_2/dark). The analytical determination evaluated for all experiments was the color removal (%).

- Characterization of TiO_2 after photocatalytic treatments

The crystallization behavior of the TiO_2 after the treatments was analyzed by X-ray diffraction (XRD) using a SIEMENS D-5000 X-Ray Diffractometer by grazing incidence technique at 1.5 degrees of incidence angle. The surface morphological features of the films were observed using a scanning electron microscope JEOL JSM-6300 (13).

- Absorption spectrum analysis

Efficient discoloration was confirmed by UV-VIS spectroscopy showing a general decrease in dye absorption (in the 200- to 800 nm region) during the treatments. The times evaluated were: 24, 48, 72 and 96 h in the biological treatment and 1, 7 and 14 h for the photocatalytic treatment (sequential treatment and only photocatalysis). Additionally, the RB5 without treatment was used to compare with the other samples.

Acute toxicity tests with Hydra attenuata

The toxicity of the dye was compared with the toxicity of the solutions before and after the biological treatment (*T. versicolor*), sequential treatment (*T. versicolor*/TiO_2UV) and photocalytic treatment by itself (TiO2/UV). In these experiments the organism used was *Hydra attenuata*, the methodology evaluated was reported by Cáceres and Bohórquez (20).

Results and Discussion

Immobilization of fungal biomass

67 ± 2.3 mg mg^{-1} of *T. versicolor* biomass was obtained using LCS as a support. This material is a porous natural fiber that allowed the colonization of *T. versicolor* by apical hyphal extension. The hyphae colonized the surface of the medium without reaching the deepest areas. This could be caused by a lower oxygen concentration in those places, generating a concentration gradient that probably affected the growth and ligninolytic enzyme production. Some authors claim that oxygen acts as a final electron acceptor in the catalytic cycle of peroxidases and laccase, establishing that both growth and production of metabolites can be inhibited if the oxygen concentration is considerably low (9, 21).

In contrast with other authors who have used polyurethane foam as immobilization carrier, the amount of biomass immobilized on this non-inert support (LCS) was higher. With polyurethane foam, the amount of biomass retained was 49 mg and 30 mg mg^{-1} for *T. versicolor* and *P. chrysosporium* respectively in the same period of culturing time (22). The reason for the better response is related to the chemical composition of the LCS, which has lignin, cellulose and hemicellulose. These are polymers which are usually degraded by the fungus in its natural habitat (23, 24). As a result, the activation of two enzymatic systems could be triggered. These enzymes are related to the lignin degradation and the hydrolysis of polymers with glycosidic linkages, induced in a complementary way. Taking this into account, it can be assumed that the fungus was able to obtain low molecular weight compounds such as cellobiose, glucose, arabinose, xylose, among others, which were used to support the primary metabolism (24).

The scanning electron microscopic micrographs of the support without biomass (LCS) can be shown in Fig. 1A, it identifies the LCS is a fibrous porous material with high surface area that favors the colonization of *T. versicolor* hyphae. In regards to the support colonized with fungal biomass, Fig. 1B reveals the thin and septate hyphae of *T. versicolor*; which cause different transformation on the surface of the LCS by the production of extracellular enzyme such as laccase. This type of structural change in lignocellulosic materials has been observed through cytochemical studies when basidiomycetes degrade lignin to mineralize it to carbon dioxide and water (25). On the other hand, in a report related with the colonization of the *Fomes sclerodermus* hyphae, the hyphae can be seen invading wooden blocks of *Poplar*, causing thinning of the walls and degradation of the parenquimatic tissue (30). This represents a similar behavior to that observed in this study, due to the fact that LCS fibers became thinner as the colonization with fungal mycelium increased.

Biological removal in bubble column reactor and operational conditions

According to the results, *T. versicolor* immobilized in LCS and under non-sterile conditions decreased the concentration of the RB5 and decolorized it efficiently. The discoloration began from the first 24 h reaching rates of 98% at the 4 d of treatment, (294 mg l^{-1}). These values remained relatively constant until the 7 d (Fig. 2).

The possible mechanisms involved in the removal of the dye could be linked to two complementary processes. The first one can be linked to the adsorption capacity of the fungal wall, which can act as a natural bio-asorbent due to the presence of chitin and certain functional groups such as amino, carboxyl and phosphate. This facilitates the removal of the dye without involving the primary metabolism (22). In the second process, the dye was bio-transformed by the action of the extracellular enzyme laccase which is induced by the presence of aromatic compounds that have structural similarity with the lignin polymer. This suggests that this process is dependent on the metabolism. Therefore, it is necessary to use a simple carbon source such as glucose to support the primary metabolism while the transformation of the aromatic compound takes place (24).

The removal obtained in the biological treatment was in some measure cause by the adsorption capacity of the LCS. This material is rich in cellulose and the dye is designed to bind tightly to the cellulose fibers via covalent bind (1). Thus, the

discoloration ability of the support material was evaluated just as an abiotic system. It was found that the material removed 31% at 24 h with a maximum of 53% until the 7 d (Fig 2.).

Under these conditions the removal of dye from the support was important. However, it does not exceed the one developed by the biological system. Highly significant differences were found ($p<0.0001$) that demonstrated that the system composed by both LCS and fungal biomass were better than the support without biomass. In contrast to Libra and Borchert who obtained a discoloration percentage of 98% in the 8th day of treatment, in this study we obtained the same discoloration percentage in the 4th d of treatment using the same dye and other strain of *T. versicolor* (8).

In relation to the discoloration obtained and its correlation with laccase production (Fig. 3). It was observed that the activity increased from the first 24 hours with values of 1 U l^{-1}, reaching a maximum value of 8 U l^{-1} at 3 d. This shows a positive correlation with the percentage of discoloration ($p=0.048$). The apparent change in color during the 7 d of treatment, ranging from black, purple, red and yellow, represent a transformation of the auxochrome-chromophore complex, which can be associated with an enzymatic attack of the hydroxy group of the dye (27). At the end of the removal kinetics, the enzymatic activity decreased dramatically. This can be related with extracellular proteases that can break down the other enzymes in the last stages of the process, where there was a deficit in the carbon or nitrogen source. Similar results were found when *P. crhysosporium* was cultured in solid fermentation using sugarcane bagasse (28).

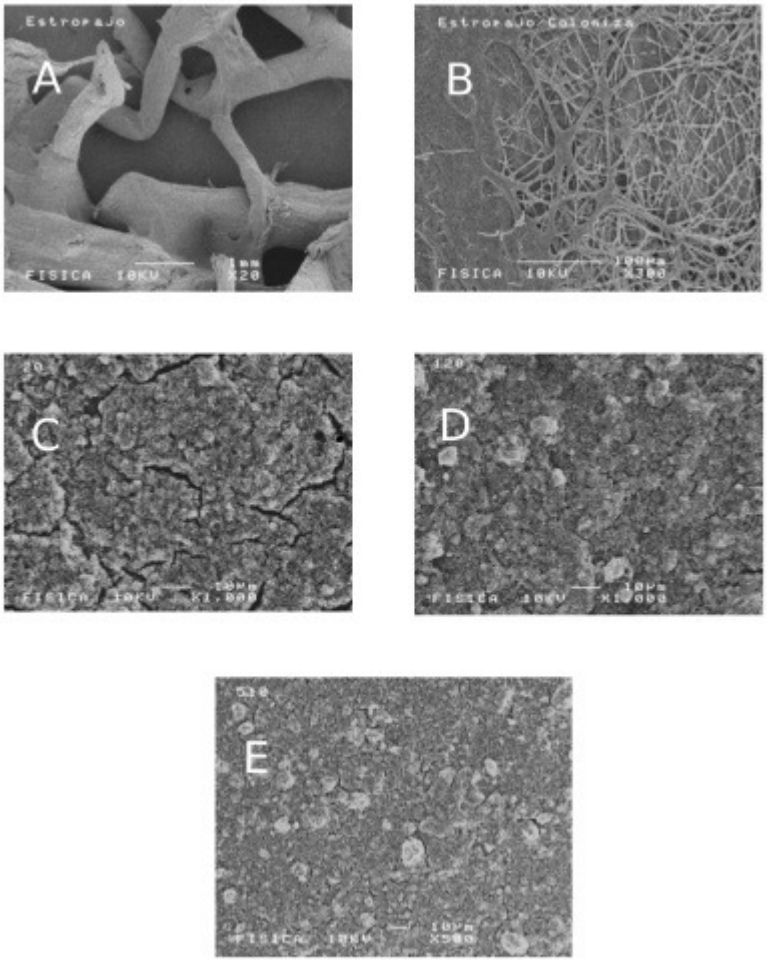

Figure 1. Scanning electron micrographs (20x) *Luffa cylindrica* without colonized (A) *Luffa cylindrica* without colonized (B) colonized mycellium of *T.versicolor* 8 d, 25°C, pH 6.5 300X. (C) titanium dioxide at 20 min (1000x), (D) titanium dioxide at 1 h (1000x) and (E) titanium dioxide at 7 h (500x) after the photocatalytic treatment in quartz reactor.

Concerning the behavior of glucose consumption and pH over time (Fig. 3), the reducing sugar was used as carbon source. There was a remarkable reduction of the glucose from 2 g l^{-1} to 0.3 g l^{-1} in period of 7 d. This can be explained by the fact that the fungus needs a simple carbon source for maintaining the primary metabolism, while it biotransforms the dye and more simple aliphatic intermediates are formed. The necessity of supplementing the mediums with a carbon source has been reported by several authors, and it has been accepted that there is a direct relation between the concentration of the substrate and the percentage of discoloration. It can be positively correlated with the enzymatic activity (9). The pH fluctuated between 4.0 and 5.0 during the 7 d of treatment due to the organic acid production in the glucose metabolism. This favored enzyme activity, since the optimal values range for activity is between 4.5 and 5.0 (30).

Photocatalytic removal with TiO_2 to sequential treatment and photocatalytic treatment without biological treatment

- Selection of the TiO_2 concentration and wavelength

According to the variance analysis for discoloration percentage (Table 1) the interaction of x_1 (254 nm) in its lower level and x_2 (1% w/v TiO_2) in its upper level has a highly significant effect on the response variable ($p<0.0001$). Under

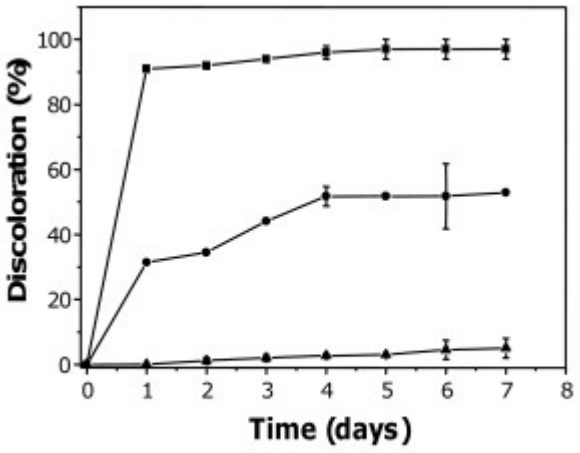

Figure 2. Discoloration of RB5 dye *T. versicolor* immobilized in LCS (■), abiotic treatment with *L. cylindrica* uncolonized (●) and absolute control (▲). 8 d, 25°C, 1 l min^{-1} flow air, under non sterile conditions.

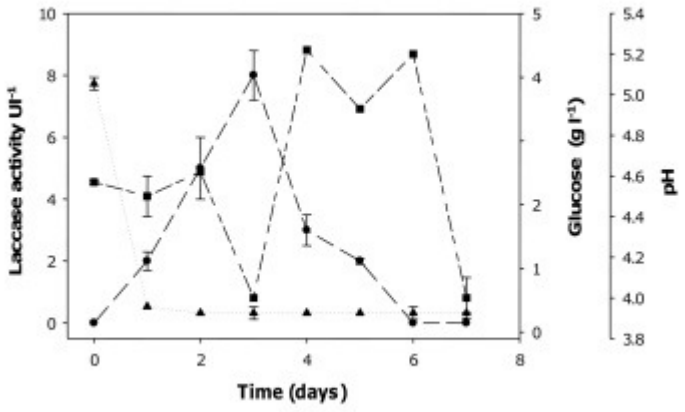

Figure 3. Time course for production of laccase activity (■), consumption of glucose (●) and pH (▲) by T. versicolor immobilized in presence of *NR5* 7 d, 25oC, 1 l min^{-1} air flow.

these conditions a discoloration of 20% after 20 min of treatment in 1 ml quartz cells was obtained. The regression equations obtained showed that each dependents variable may be predicted by following models (equation 7).

$$Discolorization(\%) = +11.1 - 5.8\,x_1 + 1.6\,x_2 + 2.3\,x_1 x_2$$

Equation 7

With respect to an x_1 factor that corresponds to the wavelength, the results showed that at 254 nm, a higher energy (4.8 eV) was provided to the forbidden band of the TiO_2 which facilitated the excitation process of the semiconductor oxide, enabling the promotion of electrons from the valence band to the conduction band (31).

On the other hand, at 366 nm, the discoloration was 7% and 10% with 0.5 and 1.0% (w/v) of TiO_2 respectively. These results might have occurred because the spectral response of TiO_2 is active in the ultraviolet region, due to the band gap (indirect transition) between the anatase and rutile phases (3.23 eV and 3.02 eV). Therefore, this determined that when evaluated at 366 nm (3.38 eV), it would work with wavelengths very near to the visible spectrum > 400 nm (3.10 eV) in which the efficiency of TiO_2 decreased and as a consequence and the discoloration was significantly lowered (12).

The positive effect of the high level of TiO_2 (x_2) was associated with an increase in the concentration of the semiconductor oxide. This facilitates a significant increase in the amount of active sites, so that the process of excitation by incident photons is carried out, and consequently causing the generation of significant amounts of reactive pairs e^-/h^+.

The discoloration percentages obtained on the small scale were not as high as the results reached in the reactor. The possible cause is the deficiency in the oxygen concentration as final acceptor of the photogenerated electrons, since the mixture of TiO_2 and effluent remained agitated only during the adsorption/desorption stabilization period. Later, when the mixture was placed in the quartz cell, no additional agitation was provided and the TiO_2 could settle. Some authors believe that one of the critical operational parameters for this type of advanced oxidation process in an adequate supply of oxygen to minimize the recombination process. Similarly, low levels of O_2 decrease the possibility of photocatalysis reductive species formation, such as $O^{\bullet-}_{2(ads)}$, $O^{2-}_{2(ads)}$ and H_2O_2, which could actively participate in the transformation of the dye (31).

- Kinetics in photocatalytic reactor

- - Photocatalysis as a post-treatment or sequential treatment

The photocatalytic system results as a post-treatment to the biological system are shown in Fig. 4. The maximum discoloration was 78% at 14 h, starting with a RB5 concentration of 6 mg L^{-1} at pH 4.1. Under these conditions, the discoloration was 21% lower than that obtained for photocatalysis as a single treatment. The decrease in the percentage may be related to the low initial concentration of the dye, which would favor the recombination process of the e^-/h^+ pairs. An analysis in terms of overall efficiency when treating the dye RB5 with the sequence *T.versicolor*/TiO_2UV after 4 d and 12 h yields a result of 99% discoloration, RB5 concentration 297 mg l^{-1} and 221 UC.

In spite of being interesting results the implementation of a combined system is definitely not a suitable option to follow for

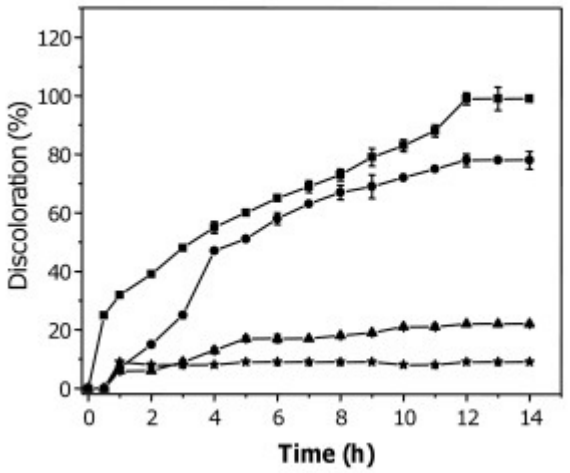

Figure 4. BR5 discolorationdiscoloration: (■) TiO_2UV, (●) *T. versicolor*/TiO_2UV, (▲) UV, (★) TiO_2 in dark. 14 h, 120 rpm, pH 4.5.

this dye, since the biological treatment depends on the physiological state of the strain, substrate consumption and co-activation of the enzyme system. Factors involving increased treatment time in the reactor and given the very high daily volumes of colored water produced in the textile industry, it would involve the installation of large storage tanks to hold water while the biological system is carried out. In contrast by using photocatalysis as unique treatment, the rates of discoloration reached are superior with a time of 12 h. However, the units of color continue beyond the maximum allowed for domestic and commercial water reuse at 75 and 20 cobalt-platinum units (32). Therefore, there should be either implemented another complementary treatment or an optimization of this treatment should be performed to achieve greater discoloration.

- - Photocatalysis as a single treatment

The highest percentages were obtained when 300 mg l-1 of RB5 was only subjected to the photocatalytic system, reaching 99% discoloration (297 mg l-1) at 12 h (Fig. 4). This difference can be attributed to the dye concentration, in which a progressive increase of it, favors the photocatalytic reaction to certain levels at which the effect is the opposite. Essentially, because the color blocks the passage of photons, and a big part of the dye could be adsorbed by the TiO2 blocking the formation of reactive pairs e-/h+, it was determined that the oxidative and reductive stages may not be carried out. Under the evaluated conditions, the possible reaction of photocatalytic mineralization that was carried out for the 300 mg l-1 of RB5 is presented in equation 8:

$$C_{26}H_{21}N_5O_{19}S_6Na_4 + 38O_2 \rightarrow 26CO_2 + 4H_2O + 4NaNO_3 + 6H_2SO_4$$

Equation 8

According to the literature review, it is assumed that the reactive species involved were of two types: It is considered that acidic pH (solution for the RB5, pH 4.5) makes the titanium surface positively charged, determining that an electrostatic attraction is present with the anionic fraction of the dye (the sulphonic groups). Under these conditions, the main oxidizing species involved could be the photogenerated holes, as indicated by the equation 1. The second species would be the electrons in the conduction band that reduced the O_2 supplied to facilitate the formation of reductive species such as $O^{\bullet-}_{2(ads)}$, $O^{2-}_{2(ads)}$ and H_2O_2. Konstantinou and Albanis suggest that the presence of aminobenzene sulfonate as a reduced intermediary demonstrates the possibility of degradation under these conditions. However, the obtained results indicate that this posibility can not be confirmed, due to the fact that the intermediaries were not quantified directly (12).

Concerning to the degradation intermediaries and their possible mineralization, some compounds can be formed: aromatic intermediaries (phenols, aromatic amines, quinones, and others) and aliphatic intermediaries (fumaric acid, succinic acid, formic acid, acetic acid, oxalic and malic acid). Finally, the group of tricarboxylic acids would be mineralized to CO_2 by a photo Colbert reaction, in which the h^+ would participate. In relation to the ions released during the process, NO^-_3, N_2 y SO_4^{2-} could be found (31).

Finally, in the photolysis and adsorption kinetics showed in Fig. 4, the UV light had a discoloration of 22% at 14 hours of treatment. By adsorption of TiO_2 in the dark, discoloration does not exceed 8.5% in the same amount of time. For this reason, the higher discoloration is associated with photocatalytic processes. This data is similar to those reported in literature by authors like Aguedach *et al*., who demonstrated that using photolysis in RB5 degradation is lower than the titanium in the absence of light which has a low adsorptive capacity. Thus, the excitation of the semiconductor oxide by the ultraviolet light is required (34).

- - Scanning electron microscopy and x-ray diffraction for the TiO_2

Scanning electron microscopy for TiO_2 (Degussa P-25) used in photocatalysis post-biological treatment is showed in Figs. 1C, 1D and 1E. At 20, 120 and 510 minutes there were no changes in the TiO_2, presenting a uniform material with some aggregates of TiO_2 that might be related to the concentration used (1% w/v) (12). Similarly, the fractures presented in some zones corresponded to the material distribution on the substrate,

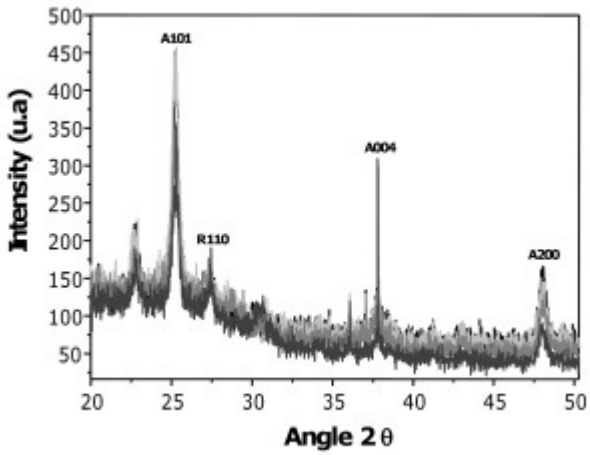

Figure 5. XRD patterns of TiO_2 after the photocatalytic treatment in quartz reactor. 14 h, 120 rpm and pH 4.5. Black lines, initial TiO_2; light gray lines, TiO_2 20 min. Tx. photocatalytic; gray lines, TiO_2 1 h Tx. photocatalytic; dark gry lines, TiO_2 7 h. photocatalytic.

because additional treatment was not applied for adhering TiO_2, only deposited over glass plate and subsequently dried out at room temperature. The analysis of X-ray diffraction showed the TiO_2 before any treatment and in each of the evaluated times, revealing the presence of the anatase phase with (101), (004) and (200) plane reflections and the rutile phase with a (110) plane reflection (Fig. 5). The largest proportion of anatase is due to the commercial composition of commercial TiO_2 Degussa-P25 which is 80% of this phase and 20% rutile. It should be noted that as time passed, the intensity of the peaks remained approximately constant suggesting that an adsorption of certain final biological-degradation products was not presented that could affect the crystallinity of TiO_2.

Table 1. ANOVA results for the selected factorial model.

Treatments	Factor x_1 Wavelength	Factor x_2 TiO_2 concentration	Observed value	Predict value
			Discoloration (%)	Discoloration (%)
1	-1	-1	14	13
2	-1	-1	12	13
3	-1	-1	13	13
4	+1	-1	7	6
5	+1	-1	5	6
6	+1	-1	6	6
7	-1	+1	20	21
8	-1	+1	21	21
9	-1	+1	22	21
10	+1	+1	5	4.67
11	+1	+1	5	4.67
12	+1	+1	4	4.67

Factor x_1: High level (+) 366 nm. Low level: (-) 254 nm.
Factor x_2: High level: (+) 1% w/v. Low level: 0.5% w/v.

Factor	Coefficient	*p* value
Intercept	11.7	<0.0001
x_1 (time)	-5.83	<0.0001
x_2 (voltage)	0.0002	1.67
x_1x_2	<0.0001	- 2.33

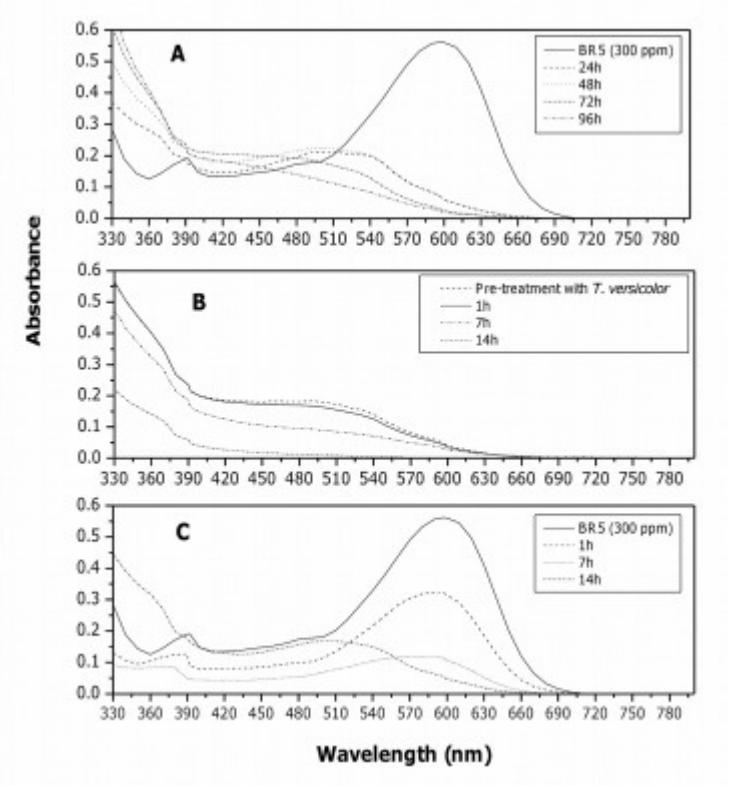

Figure 6. UV-VIS spectra of RB5 (A) Pre-treatment with *T. versicolor* immobilized in LCS, (B) sequential treatment *T. versicolor*/TiO_2UV and (C) only TiO_2UV.

Absorption spectrum analysis.

The dye discoloration was accompanied by a change in the absorption spectrum of the medium when it was treated with *T. versicolor* immobilized in LCS. The maximum absorption range shifted from the visible to UV, showing that discoloration was due to change in the dye chemical structure through enzymatic activity (Fig. 6A). The change was more evident over the course of treatment. At 48 h the absorption peak was at 512 nm and it disappeared completely at 72 h, which suggests the bio-transformation of the dye. Borchert and Libra made the same type of analysis, showing similarities with this study. The wavelength displacement of visible light to UV light is due to changes in the chemical structure of the dye. The evidence of the presence of aromatic metabolites in the degradation product can suggest a possible compound toxicity by the presence of aromatic amines (8).

The visible absorption spectrum analysis of the sequential treatment *T. versicolor*/TiO_2UV showed that absorption peaks were not registered for any of the wavelengths tested. On the other hand the changes in the 7th and 14th h could be related to the photocatalytic oxidation of some metabolites produced by *T. versicolor* after 4 days of incubation in bubble column reactor (Fig. 6B). The last scan was performed with samples that correspond only to RB5 (300 mg l^{-1}) photocatalysis, obtaining a

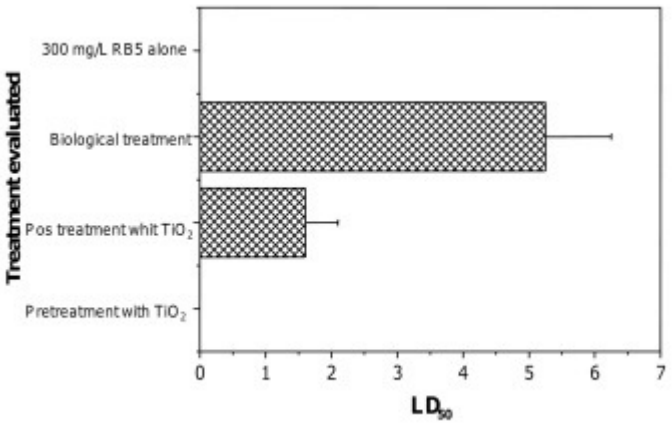

Figure 7. LD_{50} using *Hydra attenuata* such as indicator organism.

degradation of the dye by the displacement of the maximum absorption peak of 597 nm to 527 nm at 14 h. In regards to the UV spectrum, there was no significant increment. This can suggest a complete mineralization. However to confirm these results would be necessary to carry out complementary tests to observe that products were formed during the 14 h of treatment. In the photocatalytic treatment the bonds that join the azo group (chromophore) with the naphthalene rings (auxochromic group) and the bonds between naphthalene and sulfate were proposed as cutting sites, resulting in reduced time and much more aggressive dye removal (Fig. 6C) (12).

Bioassays with Hydra atenuatta

Fig 7 presents the results obtained in the bio-assay. It was demonstrated that both the biological treatment (4 d) and the sequential treatment (*T. versicolor*/UVTiO_2) were toxic to *H. atenuatta.* On the contrary, neither the dye without treatment (300 mg l^{-1}) nor the photocatalytic treatment was toxic for the organism to any of the concentrations evaluated.

The possible presence of toxic intermediaries from the biological degradation process could be responsible for the toxicity, taking into account that the absorption spectrum revealed i a spectral displacement towards the UV region. This is reported by some authors as a possible indication of the presence of aromatic compounds (8, 35), such as aromatic amines, believed to be toxic compounds. Tauber *et al.,* discusses the toxicity of the biological degradation products of reactive black five, based on the inhibition of the respiratory rate of *Pseudomonas putida*, finding a small RB5 toxicity increase after 6 h of treatment. Nevertheless, the dye treated with photocatalysis in this work did not appear to be toxic after 14 h of treatment. This result agrees with the absorbance analysis since the absorption peak is not displaced to the UV region (35). Reutergárdh and Iangphasuk conducted the toxicity analysis of RB5 after 120 min of photocatalytic treatment, determining that the toxicity decreases considerably after treatment. However, this study found that Reactive Black Five (300 mg l^{-1}) did not present toxicity to *H. attenuata* (35).

Conclusions

In all of the valuated process important results were obtained. *T. versicolor* removed the dye RB5 up to 4 days of treatment under non-sterile conditions, showing that there is a direct correlation with the production of ligninolytic enzymes such as MnP and laccase. However, the mineralization was not complete and aromatic intermediaries could be formed and these intermediaries possibly caused a toxic effect on *H. attenuata.*

The results of the photocatalytic treatment demonstrated that both the sequence *T. versicolor*/ TiO_2UV and photocatalysis as a single treatment were efficient options for azo dye removal. However, when the dye is only treated with TiO_2/UV, the removal was higher and took less time. As an additional advantage the obtained effluent under these conditions was not toxic to the evaluated organism.

Acknowledgments

This work was supported in part by Universidad Javeriana. Project No. 2730. We are grateful to Dr. Ciro Falcony-Guajardo, Dr. Refugio Rodriguez Vázquez and Ms. Ana Bertha Soto Guzmán for performing the electron microscopy work. Departamento de Física. Departamento de Biotecnología y Bioingeniería. Centro de Investigación y Estudios Avanzados. Instituto Politécnico NAcional (Cinvestav-IPN). Avenida Politecnico Nacional 2508. México.

References

1. **McMullan G, Meehan C, Conneely A, Kirby N, Robinson T, Nigam P, Banat IM, Marchant R, Smyth WF** (2001) Microbial discoloration and degradation of textile dyes. Appl Microbiol Biotechnol 56:81–87
2. **Levin L, Papinutti L, Forchiassin F** (2004) Evaluation of Argentinean white rot fungi for their ability to produce lignin modifying enzymes and decolorize industrial dyes. Bioresour Technol 94:169–176
3. **Banat IM, Nigam P, Singh D, Marchant R** (1996) Microbial discoloration of textile-dye-containing effluents: a review. Bioresour Technol 58:217–225
4. **Chander M, Arora DS** (2007) Evaluation of some white-rot fungi for their potential to decolourise industrial dye. Dyes Pigm. 72:192–198
5. **Nilsson I, Möller A, Mattiasson B, Rubindamayugi MST, Welander U,** (2006) Discoloration of synthetic and real textile wastewater by the use of white-rot fungi. Enzyme Microb Technol 38:94–100
6. **Romero S, Blánquez P, Font X, Gabarrell X, Sarrá M, Caminal G, Vicent T** (2006) Different approaches to improving the textile dye degradation capacity of *Trametes versicolor.* Biochem Eng J 31:42–47
7. **Song S, He Z, Qiu J, Xu L, Chen J** (2007) Ozone assisted electrocoagulation for discoloration of C.I. Reactive Black 5 in aqueous solution: An investigation of the effect of operational parameters. Sep Purif Technol 55:238–245
8. **Borchert M, Libra J**A (2001) Discoloration of reactive dyes by white rot fungus *Trametes versicolor* in sequencing batch reactors. Biotechnol Bioeng 75:313–321
9. **Durán N, Rosa MA, D'Annibale A, Gianfreda L** (2002) Applications of Laccases and tyrosinases (phenoloxidases) immobilized on different supports: a review. Enzyme Microb Technol 31:907–931
10. **Shin M, Nguyen T, Ramsay J** (2002) Evaluation of support materials for the surface immobilization and decoloration of amaranth by *Trametes versicolor.* Appl Microbiol Biotechnol 60:218–223
11. **Zille A, Górnacka B, Rehorek A, Cavaco-Paulo A** (2005) Degradation of azo dyes by *Trametes villosa* laccase over long periods of oxidative conditions. Appl Environ Microbiol 71:6711–6718
12. **Konstantinou IK, Albanis A** (2004) TiO_2-assisted photocatalytic degradation of azo dyes in aqueous solution: kinetic and mechanistic investigations: A review. Appl Catal B 49:1–14
13. **Pedroza-Rodríguez AM, Mosqueda R, Alonso-Vante N, Rodriguez-Vazquez R** (2007) Sequential treatment via *T. versicolor* and UV/TiO_2/Ru_xSe_y to reduce contaminants in waste water resulting from the bleaching process during paper production. Chemosphere 67:793–801
14. **Radha KV, Regupathi I, Arunagiri A, Murugesan T** (2005) Discoloration of synthetic dyes using *Phanerochaete chrysosporium* and their kinetics. Process Biochem (Amsterdam, Neth) 40:3337–3345
15. **Miller G** (1959) Use or dinitrosalicilic acid reagent for determination of reducing sugar. Anal Chem 35:.426–428
16. **Tinoco R, Pickard MA, Vazquez-Duhalt R** (2001) Kinetic differences of purified laccase from six *Pleurotus ostreatus* strains. Lett Appl Microbiol 32:331–335
17. **Michel F, Balachandra S, Grulke E, Adinarayana C** (1991) Role of manganese peroxidases and lignin peroxidases of *Phanerochaete chrysosporium* in the discoloration of kraft bleach plant effluent. Appl Environ Microbiol 57:2368–2375
18. **Tien M, Kirk TK** (1988) Lignin peroxidase of *Phanerochaete chrysosporium*. Methods Enzymol 161:238–249
19. **Montgomery DC** (2003) Diseño y análisis de experimentos. Editorial Limusa-Wiley, México D.F, pp. 218
20. **Cáceres L, P. Bohórquez P** (2002) Puesta a punto de una bateria de bioensayos con *Hydra attenuata*, *Daphnia magna*, *Lactuca sativa* y *Allium* cepa para evaluar toxicidad en agua. Degree Thesis (Microbiología Industrial). Universidad Javeriana. Bogotá, Colombia, pp. 133
21. **Dávila A, Vázquez-Duhalt R** (2006) Enzimas ligninolíticas fúngicas para fines ambientales In O Flores-Herrera, I Velasquez-lópez E Rendón-Huerta J Oria-Hernández, eds, Mensaje Bioquímico, Vol 30. Facultad de Medicina-UNAM, México DF, pp 29–55
22. **Gómez-Bertel S, Amaya-Bulla D, Maldonado-Saavedra C, Martínez-Salgado MM, Quevedo-Hidalgo B, Soto-Gúzman A, Pedroza-Rodríguez** AM (2008) Evaluación de *Phanerochaete chrysosporium, Trametes versicolor*, *Pleurotus ostreatus* y *Aspergillus niger* como alternativa para el tratamiento de aguas residuales del curtido de pieles. Rev Int Contam Ambient 24:93–106
23. **Papinutti VL, Diorio LA Forchiassin F** (2003) Degradación de madera de álamo por *Fomes sclerodermeus*: producción de enzimas ligninolíticas en aserrín de álamo y cedro. Rev Iberoam Micol 20:16–20
24. **Arora DS, Gill PK** (2000) Laccase production by some white rot fungi under different nutritional conditions. Bioresour Technol 73:283–285
25. **Garcia S, Large J, Prevost MC, Leisola W** (1987) Wood Degradation by White Rot Fungi: Cytochemical Studies Using Lignin Peroxidase-Immunoglobulin-Gold Complexes. Appl Environ Microbiol 53:2384–2387
26. **Camarero S, Ibarra D, Martínez MM, Martínez A** (2005) Lignin-Derived Compounds as Efficient Laccase Mediators for Discoloration of Different Types of Recalcitrant Dyes. Appl Environ Microbiol 71:1775–1784
27. **Couto S, Gudín M, Lorenzo M, Sanromán MA** (2002) Screening of supports and inducers for laccase productions by *T. versicolor* in semi-solid-state conditions. Process Biochem (Amsterdam, Neth) 38:249–255

28. **Cruz-Córdoba T, Roldán-Carrillo TG, Díaz-Cervantes D, Ortega-López J, Saucedo-Castañeda G, Tomasini-Campocosio A, Rodríguez-Vázquez R** (1999) CO_2 evolution and ligninolytic and proteolyticactivities of *Phanerochaete chrysosporium* grown in solid state fermentation. Resour, Conserv Recycl 27:3–7

29. **Tavares A, Coelho M, Coutinho J, Xavier A** (2004) Laccase improvement in submerged cultivation: induced production and kinetic modeling. J Chem Technol Biotechnol 80:669–676

30. **Pazarlioğlu NK, Sariişik M, Telefonku A** (2005) Laccase: Production by *Trametes versicolor* and application to denim washing. Process Biochem (Amsterdam, Neth) 40:1673–1678

31. **Carp O, Huisman C, Reller A** (2004) Photoinduced reactivity of titanium dioxide. *Prog Sol St Chem* 32:33–177

31. **Tangand C, Chen V** (2004) The photocatalytic degradation of reactive black five using TiO_2/UV in an annular photoreactor. Water Res 38:2775–2781

33. Decreto 1594 (1984) Usos del agua y residuos líquidos. Ministerio de Salud, Republica de Colombia, pp. 1–52

34. **Aguedach A, Brosillon S, Morvan, J Lhadi E** (2005) Photocatalytic degradation of azo-dyes reactive black 5 and reactive yellow 145 in water over a newly deposited titanium dioxide," Appl Catal B 57:55–62, 2005

35. **Tauber M, Guebitz G, Rehorek A** (2004) Degradation of azo dyes by laccase and Ultrasound treatment. Appl Environ Microbiol 71:2600–2607

International Biotechnology Color Journal

Physiological effects of products obtained by nixtamalization and extrusion of quality protein maize.

María del Carmen Robles-Ramírez[1], *Yesenia Acoltzi-Tamayo*[2], *Cristian Sánchez-Vega*[2], *Eliseo Sosa-Montes*[3], *Cuauhtémoc Reyes-Moreno*[4], *Jorge Milán-Carrillo*[4], and *Rosalva Mora-Escobedo*[1]*.

[1]Escuela Nacional de Ciencias Biológicas, IPN, México.

[2]Instituto Tecnológico del Altiplano de Tlaxcala, Tlax., México.

[3]Universidad Autónoma de Chapingo, Departamento de Nutrición Animal, Texcoco, Edo. de Mexico.

[4]Universidad Autónoma de Sinaloa, Facultad de Ciencias Químicas, Culiacán, Sin., México.

*To whom all correspondence should be sent.

Chief Editor: José J. Zúñiga-Aguilar. Area Editor: Susana Lozano. Recieved: April 15, 2011. Revised version: September 7, 2011. Accepted: September 30, 2011.

Abstract

The effects of dietary products obtained by nixtamalization and extrusion of quality protein maize (QPM), on food conversion efficiency (FCE), fecal weight and volume, and the apparent digestibility of fiber, fat and energy, were investigated in Wistar rats and compared with a commercial brand. Eight diets were tested: unprocessed QPM flour, nixtamalized and extruded QPM flours, tortillas from nixtamalized and extruded QPM flours, commercial maize flour, commercial tortilla, and a diet of casein with 5 % cellulose as control. Food conversion efficiency was higher in QPM products compared to commercial. The processing did not reduce the nutritional value of QPM: extruded QPM flour showed higher food conversion efficiency than unprocessed QPM flour ($p<0.05$) whereas nixtamalization did not produce significant changes ($p=0.30$). Digestibility of nutrients studied and fecal bulk were related to fiber content and type of process. QPM extruded products showed higher ($p<0.05$) fiber content, weight and volume of feces, and lower ($p<0.05$) fiber, fat and energy digestibility, than QPM nixtamalized products and commercial brand. Tortillas preparation did not cause changes in fiber content of maize products ($p>0.05$). These results showed that extruded QPM flours, besides providing good quality protein, supplies a significant proportion of fiber, which has beneficial effects on health.

***Contact address:** Dr. Rosalva Mora Escobedo. Escuela Nacional de Ciencias Biológicas, IPN. Prolongación de Carpio y Plan de Ayala S/N, Col. Sto. Tomás, México, D.F. C.P. 11340. Tel.: 52-5557296000 Ext. 62462. Fax: 52-5557296000, Ext. 62463 e-mail: *rosalmora@hotmail.com*

Keywords: Quality Protein Maize (QPM), fiber, extrusion, nixtamalization, digestibility.

Abbreviations: QPM, quality protein maize obtained by traditional genetic improvement; FCE, food conversion efficiency; RS, resistant starch; RH, relative humidity.

Yellow: Nutritional Biotechnology

Introduction

The interest in dietary fiber has increased in recent decades and the importance of this food constituent has led to the development of a large market for fiber-rich products (1). Fiber is an important component of food, that has attracted the attention of nutritionists and food specialists, initially due to the epidemiological studies that related diet fiber deficiency with gastrointestinal disorders, obesity, cardiovascular diseases and diabetes. However, accumulated evidence indicates that fiber-rich foods may function as normal dietary agents, by modulating the digestive and absorptive process. Physical and chemical properties of fiber sources (water retention capability, viscosity, organic molecules absorption, cation exchange and large intestine fermentation) are important in the determination of their physiological responses such as increased fecal bulk, modulation of the rates of nutrient digestion and absorption, reduced levels of cholesterol in plasma and reduced glycemic responses to diet (2).

The high consumption level of maize products in developing countries has encouraged the development of new processing methods to improve functionality and nutrient quality of maize-based products (3).

Nixtamalization is the alkaline boiling process of maize that has been put into practice in Latin America since the pre-Columbian era. A dough known as "masa" is obtained from the milling of nixtamalized maize and utilized to prepare "tortillas", "atoles", "tamales" and other regional dishes. This procedure reduces starch content, but increments the content of soluble fiber and resistant starch (RS); the last parameter rises when consumers store tortillas and heat them again (4, 5).

A step forward in nixtamalization technology in recent years has been the production of flours with a larger shelf life, simplifying the elaboration of home made "tortillas" (6). However, the traditional nixtamalization process to produce instant flours consumes time and energy, and generates high volumes of contaminant effluents (3-10 l H_2O/kg of maize). Extrusion represents a technological alternative to the production of flours, without the generation of polluted effluents (7). Optimal parameters for an extrusion process in the production of instant flour of QPM (quality protein maize obtained by traditional genetic improvement) have been determined, resulting in a product with physicochemical and functional characteristics similar to the commercial nixtamalized maize flours (7, 8). It has been found that there is an increment of resistant starch during the production of instant QPM flour by nixtamalization and extrusion, and there is an additional increment during the production of tortillas made of these flours, therefore increasing the fiber content of these products (9).

Some studies carried out with several cereals as barley, wheat and maize have revealed an increment in fiber content and higher food conversion efficiency after they were processed by extrusion (10-14). For instance, Martínez *et al.* (11) reported, for commercial maize products, an increase of 36.2% in dietetic fiber of "tortillas" made from fresh masa extruded with 0.25% lime, with regard to raw maize flour. However, there are few studies related to the influence of thermal, chemical and mechanical processes, utilized in the production of maize products, on fiber content and physiological response to ingestion of quality protein maize; thus, the aim of this work was to determine the physiological response (weight and volume of feces as well as the fiber, fat and energy digestibilities) of rats to fiber of QPM products, obtained by nixtamalization and extrusion processes.

Materials and methods

Materials

White QPM (Zea mays L, cv. V-537C) was grown under irrigation and fertilization conditions at the Culiacan Valley Experimental Station of INIFAP, Culiacan, Sinaloa, Mexico. The materials tested were: unprocessed, nixtamalized and extruded QPM flours; tortillas made with nixtamalized and extruded QPM flours; commercial maize flour and commercial tortilla.

Preparation of nixtamalized maize flours

The production of instant QPM nixtamalized flours was carried out using the methodology reported by Milan-Carrillo et al. (15). Briefly, 100 g maize were soaked in a solution of 5.4 g $Ca(OH)_2$/L at 85 ºC. The ratio of grain to cooking medium was 1:3 and the nixtamalization and steep times were 31 min and 8.1 h, respectively. Alkaline-cooked maize kernels were washed with running tap water and then dried (24 h, 55 ºC) and milled to pass through 80-US mesh screen.

Preparation of extruded maize flours

The production of instant flour from quality protein maize (QPM) was assessed according Milán-Carrillo et al. (8). Prior to extrusion, the maize kernels were broken to obtain grits (1 to 2 mm) which were mixed with lime (0.21 g lime/100 g maize) and water to reach a moisture content of 28 g/100 g. The extrusion was carried out with a single-screw laboratory extruder (Brabender model 20 DN, NJ, USA) with a 19 mm screw-diameter, length-to-diameter 20:1, nominal compression ratio 2:1, and die opening of 2.4 mm; and the extrusion conditions were: 85 °C, and screw velocity of 240 rpm. Extrudates were cooled, dried at environmental conditions (25 °C, 65% RH) for one day, and milled in an UDY Cyclone Sample Mill (UDY Corp., Fort Collins, Co, USA) to pass through an 80-US mesh (0.180 mm) screen, packed in plastic bags, and stored at 4 °C.

Preparation of "tortillas" from nixtamalized and extruded maize flours

"Tortillas" were prepared by mixing 200 g of maize flour with sufficient water to reach an adequate consistency, for the production of tortillas. The fresh "masa" (30 g/tortilla) was rounded and shaped into the form of flat disk using a manual machine. The "masa" disks were baked on a hot griddle at 290 ± 10°C for 27 sec on one side, followed by 30 sec on the other side, and then turned back on the first side until puffing. Samples of fresh tortilla were air-dried at room temperature, milled, and stored at 4 °C in polyethylene bags, for further analysis.

Chemical analyses

The moisture content was determined by the reduced pressure method (44-15 A), crude fat by Soxhlet (30-10) and total protein by Kjeldahl (46-12) (%N x 5.85), using techniques recommended by AACC (16). Total dietary fiber was determined according to 45.4.08 AOAC method (17). The gross energy was determined in the dried samples of food and feces using a 1266 Isoperibol Bomb Calorimeter (Parr Instrument Company, Moline, Ill. USA) according to manufacturer's instructions.

Diets

Diets were composed of flour from the different maize products (8.2-10.7% protein), 2% vitamin mix, 4% mineral mix and adjusted to 10% fat with corn oil. Furthermore, a group of rats (control group) was fed with a diet containing 10% casein, 10% corn oil, 2% vitamins, 4% minerals, 5% cellulose and 69% maize starch. The vitamin and mineral mixes were AIN-93-VX and AIN-93G-MX, respectively (Harland Tekland Laboratory Animal Diets, Madison, Wi, USA).

Animal model

Experiments in animals were approved by the Laboratory of the Animal Care Committee of our Institution and were conducted in compliance with the official Mexican regulations (18). Wistar rats (ENCB Breeding Center, D.F., Mexico) were randomly distributed in groups of 10 rats for each test diet (5 males and 5 females) and housed in individual cages. Animals were maintained at 20 ± 1 °C and 55% relative humidity, under 12 h light/12 h dark cycles. An adaptation period of 7 days and a balance period of 7 days were used. The animals had free access to food and water. During the balance period feces were collected and weighed; then dried and weighed again. Body weight and food intake were also recorded. Fecal volume was assessed in a graduated test tube using sand as an embedding media.

Food conversion efficiency (FCE) was calculated as follows: Body weight gain (g) × 100/food intake (g). Fiber, fat and energy content in both, diets and feces (recollected during balance period) were determined in order to obtain digestibility. Apparent digestibility of fiber, fat and energy, were calculated as the difference of the recorded quantitative intake and excretion, expressed as percentage of ingestion.

Statistical Analysis

All data were expressed as means ± SD. Statistical comparisons were made using one-way analysis of variance (ANOVA) and significance determined with a Tukey test. Statistical significance was defined as $p \leq 0.05$. Analysis was done using Microsoft Office Excel 2003 (Microsoft, Redmond, Wa. USA).

Results and discussion

Nixtamalization and extrusion are two methods used to obtain instant flours which are used to make tortillas in Mexico. No studies have investigated the effect of these processes on both the fiber content and the physiological response of rats fed products obtained from quality protein maize, a nutritionally improved grain, rich in lysine and tryptophan, developed in Mexico. Table 1 shows the results of biological evaluation. Food conversion efficiency (FCE) was approximately two fold higher in QPM products, than in commercial products; these results agree with the better nutritional quality of QPM products (19). The process (nixtamalization or extrusion) did not diminish the nutritional value of QPM; on the contrary, the extrusion enhanced it. Extruded QPM flour had a higher FCE than unprocessed QPM flour (14.6% vs. 10.6%, $p=0.02$). Extruded QPM flour showed the best FCE, which could be due the higher biodisponiblility of lysine and protein digestibility, as Milan et al., (2006) reported. Studies with pigs showed that extruded cereals improve weight gain and FCE with respect to raw cereals (13), probably because the process of extrusion inactivates antiphysiological factors and increases the protein digestibility, which improves food nutritional properties (20, 21). On the other hand, nixtamalization process did not produce significant changes in FCE ($p>0.05$), but tortilla preparation of extruded QPM and nixtamalized QPM showed low values of FCE ($p<0.05$). This could be due to chemical reactions between proteins with carbohydrates (Maillard reactions).

Table 1. *Biological evaluation of rats fed different diets*[*].

Diet	Weight gain (g)	Total food intake (g)	Food conversion efficiency (%)
Casein (control) [**]	23.8±5.9[a]	117.3±6.3[c]	20.9±4.2[a]
Unprocessed QPM flour	13.5±4.5[c]	126.2±10.3[bc]	10.5±2.7[c]
Extruded QPM flour	21.2±2.2[b]	148.7±15.3[a]	14.6±3.1[b]
Extruded QPM tortilla	13.9±4.8[c]	139.3±13.0[a]	10.4±2.6[c]
Nixtamalized QPM flour	15.0±3.3[c]	132.3±5.2[b]	11.8±2.3[bc]
Nixtamalized QPM tortilla	15.9±5.9[bc]	140.8±10.6[a]	11.6±3.4[c]
Commercial flour	8.4±3.6[d]	119.4±10.5[c]	6.8±2.5[d]
Commercial tortilla	5.7±2.2[e]	96.8±7.8[d]	5.8±2.1[d]

[*] Results were expressed as means ± SD (n = 10). Mean values followed by different superscripts in the same column are significantly different ($p \leq 0.05$).
[**] 5% cellulose.

Table 2 shows the results of total dietary fiber of the different diets, and the fecal output in rats fed maize products. The higher levels of fiber corresponded to extruded QPM products which had values above the unprocessed flour from which they proceeded. Similar results were obtained by Martínez et al. in maize commercial products (11), who attributed the increment in fiber content to the lack of pericarp

Table 2. *Total fiber of diets and fecal output in rats fed different diets*[*]

Diet	Total Dietary Fiber (%)	Wet fecal weight (g)	Dry fecal weight (g)	Fecal volume (cm^3)	$\left(\frac{\text{wet feces}}{\text{food intake}}\right)$
Casein (control) [**]	5.3±0.3[d]	6.1±1.2[c]	5.4±0.9[c]	6.9±1.6[c]	0.05
Unprocessed QPM flour	13.2±2.0[b]	7.9±1.1[b]	6.8±1.1[b]	13.0±2.5[a]	0.063
Extruded QPM flour	15.5±1.1[a]	10.0±1.0[a]	8.5±0.9[a]	13.9±3.8[a]	0.07
Extruded QPM tortilla	15.2±0.9[a]	10.5±1.2[a]	8.9±0.9[a]	14.2±2.5[a]	0.075
Nixtamalized QPM flour	9.1±1.1[c]	5.6±0.8[c]	4.7±0.9[c]	5.5±1.7[d]	0.042
Nixtamalized QPM tortilla	9.3±1.3[c]	5.5±0.7[c]	4.6±0.5[c]	9.5±1.8[b]	0.040
Commercial flour	10.6±0.7[bc]	5.2±0.8[c]	4.5±0.7[c]	7.9±2.1[c]	0.044
Commercial tortilla	12.0±1.6[b]	3.4±0.6[d]	2.9±0.6[d]	5.7±1.9[d]	0.035

[*]Values are means ± SD (n = 10). Mean values followed by different superscripts in the same column are significantly different (p≤0.05).
[**] 5% cellulose.

removal, and to protein changes during the extrusion with lime, which produces complex polymers that become dietetic fiber. Vasanthan et al. (14) attributed the fiber increase during the extrusion of barley to the formation of soluble fiber by transglycosidation. The increment in fiber may also be due to the formation of resistant starch as a result of processing. Starch characteristics, digestibility and nutritional properties, as well as its content can be modified by an industrial hydrothermal process (22). Resistant starch (RS) is starch highly resistant to the action of amilolytic enzymes of mammals, therefore it is considered as a fiber component (22, 23). Perales et al. (24) have reported an increment in RS of approximately 1%, during instant flour production by nixtamalization and extrusion. Nixtamalized QPM products had smaller dietetic fiber content ($p<0.05$), than flours without processing, which matches the results of others studies (25). The reduction on fiber content is related to pericarp removal and hemicellulose hydrolysis that takes place during the nixtamalization process (6, 25).

The highest fecal excretion corresponded to the groups fed extruded products; extruded QPM diets (tortilla and flour) resulted in significantly higher wet and dry fecal weights as well as fecal volumes than other diets ($p<0.05$). The highest fecal output was related to higher fiber content. The formation of resistant starch (RS) during extrusion might be responsible for this physiological response, as was reported by Ranhotra et al. (23), who found that RS increases the fecal volume.

Even though the fecal weight and volume were greater in rats fed products with higher fiber content, it is important to note that food intake was also large for these diets ($p<0.05$). It could be argued that the increased production of feces was due to the increased food intake. However, when wet feces/food intake ratios were calculated, the highest values were obtained in rats fed products with the largest fiber content (Table 2). The increased intake of diets high in fiber could be due to its lower caloric density (rats should eat more in order to satisfy their energetic requirements), since dietary fiber digestibility of these diets was lower (Table 3). Additionally, the reduced retention time could decrease even more the absorption of nutrients (26).

Apparent digestibility of fiber, fat and energy are shown in Table 3. In general, fiber digestibility of maize products was remarkably greater than digestibility of control diet ($p<0.05$). This is manifested by a lower percentage of fiber excretion with respect to total intake in the groups fed maize products, due to fermentation of fiber by the large intestine microflora. The major components of maize fiber are hemicelluloses, which are 60 to 90% digestible by intestinal micro flora (27); likewise, the resistant starch formed during maize processing is also digestible to a great extent (23). The fiber digestibility values of the extruded products used were 73.1% (extruded QPM tortilla) and 75.8 % (extruded QPM flour), which are similar to the 79.5% obtained by Medel *et al*. (13) in extruded maize, for pigs.

There was no significant difference among the fiber digestibility of extruded QPM flour, extruded QPM tortilla, and unprocessed QPM flour (75.8, 73.1 and 74.3% respectively). In these QPM products, the fiber increment caused by extrusion, without increment in fiber digestibility, explains the large fecal volume. However, nixtamalization significantly increased fiber digestibility (85.8% in nixtamalized QPM flour compared to

Table 3. *Apparent digestibilities of fiber, fat and energy in rats fed different diets*[*]

Diet	Digestibility (%)		
	Fiber	Fat	Energy
Casein (control) [**]	44.8±8.8[e]	96.3±0.2[a]	95.7±0.8[b]
Unprocessed QPM flour	74.3±2.1[d]	92.7±0.7[c]	94.5±0.5[c]
Extruded QPM flour	75.8±2.2[d]	89.8±1.9[d]	94.1±0.4[c]
Extruded QPM tortilla	73.1±1.6[d]	91.2±1.3[d]	94.1±0.5[c]
Nixtamalized QPM flour	85.8±1.5[b]	94.1±1.4[b]	95.8±0.8[b]
Nixtamalized QPM tortilla	88.1±0.9[a]	93.6±0.6[bc]	96.3±0.4[ab]
Commercial flour	81.2±1.4[c]	94.6±0.8[b]	96.3±0.3[ab]
Commercial tortilla	88.7±0.7[a]	94.9±0.8[b]	96.7±0.4[a]

[*] Digestibility results were expressed as means ± SD (n=10). Mean values followed by different superscripts within the same column are significantly different (p≤0.05).
[**] 5% cellulose.

74.3% in unprocessed QPM flour; $p<0.05$), which resulted in a minor fecal weight and volume (Table 3). Probably the nixtamalization conditions (alkaline media and larger water content than in extrusion process) facilitated hemicelluloses hydrolysis, as well as the formation of soluble gum and resistant starch; products easily fermented by intestinal microflora. On the other hand, the results obtained by Kahlon et al. (28), when they studied the effect of wheat bran fiber on fiber digestibility in rats, indicated that digestibility varies significantly with the type and level of dietetic fiber. In the present work, the smallest levels of fiber corresponded to a higher digestibility, except in control diet with 5% of cellulose, which is not digestible. Fiber digestibility of the control diet (44.8 ± 8.8) was similar to that reported by Kahlon for a casein diet with 5% cellulose. The highest fiber digestibility of maize diets compared with the control diet suggests that a large part of maize fiber is soluble fiber, digestible by colon microflora. On the other hand, different studies have demonstrated that the retention time in large intestine is an important factor that influence fiber digestibility. An increment in fiber intake diminishes intestinal transit time, reducing fiber digestion (28).

Digestibility values of fat indicates that there was a significantly larger excretion of fat in the groups fed high-fiber products (unprocessed QPM flour, extruded QPM flour and extruded QPM tortillas), which had smaller values of fat digestibility (92.7, 89.8 and 91.2%, respectively) than the nixtamalized products, which presented values of approximately 96%. Wisker *et al.* (26) and Kahlon *et al.* (28) obtained fat digestibility values of 94% in rats fed with integral rye bread (7.3% of non starch polysaccharides) and 94.8% in rats fed with diets containing 20% of wheat bran (10% fiber), respectively.

Cummings *et al.* (29) in human experiments found an increment in fecal fat when the intake of dietetic fiber was increased, resulting in an increase of nitrogen, Ca, short chain fatty acids, and bile acids excretion. In an experiment with rats, Munakata *et al.* (30) found that fat excretion was larger in rats fed 15% pectin diet, followed by those that were fed 15% cellulose, than non fiber diets. Some studies have demonstrated that dietetic fiber has an inhibitory effect on gastrointestinal enzymes activity, among them, lipases. Fibers can hinder the mixing of the luminal content and delay the transport of enzymes to their substrates and of the products to the absorption surface. Viscous fibers also affect the emulsification of lipids by causing an increase in lipid droplet size and, as a consequence, a decrease in the contact surface between the lipid and aqueous phases (31). Moreover, the capacity of some fiber components to bind bile acids is also associated to the reduction of lipid absorption (2).

Although there was a small difference in the energy digestibility values among the groups, the rats fed QPM flour without processing, extruded QPM flour and extruded QPM tortilla, showed energy digestibilities significantly smaller ($p<0.05$) than the rest of the groups. This was probably due to the bigger effect of products high in fiber on fecal excretion and thus on fecal energy loss.

Conclusions

Hydrothermal processes such as nixtamalization and extrusion affect the dietary fiber content of quality protein maize and, in consequence, the physiological response of rats to this food. The extrusion process increases the fiber content probably due to the formation of resistant starch and complex polymers. Nixtamalization, on the contrary, diminished it because of pericarp removal during process. A greater fiber content in diet resulted in an increment of feces weight and volume. QPM extruded products were the highest in dietary fiber and the lowest in fiber, fat and energy digestibilities, so the only way to explain the increase in growth and food conversion efficiency of rats fed with QPM extruded products is the highest concentration of protein, better digestibility and an aminoacid balance associated with increased consumption of food. Our results showed that extruded QPM flours, besides providing good quality protein, supply a significant proportion of fiber which has beneficial effects on health of the individual who consumes it. This finding is critical, because nutritional problems afflicting the world's population are on one side the protein deficiency, but on the other side health problems associated with food as obesity, diabetes, cardiovascular disease and cancer.

Acknowledgments

This research was supported by grants from Instituto Politécnico Nacional; the COFAA-IPN and Universidad Autónoma de Sinaloa.

References

1. **Zhang M, Liang Y, Pei Y, Gao W, Zhang Z** (2009) Effect of Process on Physicochemical Properties of Oat Bran Soluble Dietary Fiber. J Food Sci 74:C628–C636
2. **Tungland BC, Meyer D (2002)** Nondigestible oligo and polysaccharides (dietary fiber): their physiology and role in human health and food. CRFSFS 1:90–109
3. **Sefa-Deheh S, Cornelius B, Sakyi-Dawson E, Ohene E** (2004) Effect of nixtamalization on the chemical and functional properties of maize. Food Chem 86:317–324

4. **García-Rosas M, Bello-Pérez A, Yee-Madeira H, Ramos G, Flores-Morales A, Mora-Escobedo R** (2009) Resistant starch content and structural changes in maize (*Zea mays*) tortillas during storage. Starch/Stärke 61:414–421

5. **Mora-Escobedo R, Osorio-Díaz P, García-Rosas MI, Bello-Pérez A, Hernández-Unzón H** (2004) Changes in select nutrients and microstructure of white starch quality maize and common maize during tortilla preparation and storage. Food Sci Tech Int 10:79–87

6. **Bello-Pérez LA, Osorio-Díaz P, Agama-Acevedo E, Nuñez-Santiago C, Paredes-López, O** (2002) Chemical, physicochemical and rheological properties of masas and nixtamalized maize flour. Agrociencia 36:319–328

7. **Reyes-Moreno C, Milán-Carrillo J, Gutiérrez-Dorado R, Paredes-López O, Cuevas-Rodríguez EO, Garzón-Tiznado JA** (2003) Instant flour from quality protein maize (*Zea mays* L) Optimization of extrusion process. Lebens Wiss u-Technol 36: 685–695

8. **Milán-Carrillo J, Gutiérrez-Dorado R, Perales-Sánchez JXK, Cuevas-Rodríguez E O, Ramírez-Wong B, Reyes-Moreno C** (2006) The optimization of the extrusion process when using maize flour with a modified amino acid profile for making tortillas. Int J Food Sci Tech 41:727–736

9. **Perales J, Gutiérrez R, Milán J, Bello L, Reyes C** (2005) Cambios en el almidón de maíz de calidad proteínica durante la producción de harinas instantáneas y tortillas. Rev Ciencia y Tec 3:150–154.

10. **Esposito F, Arlotti G, Bonifati A, Napolitano A** (2005) Antioxidant activity and dietary fiber in durum wheat bran by-products. Food Res Inter 38:1167–1173

11. **Martínez HE, Martínez F, Figueroa JD, González J** (2002) Studies and biological assays in maize tortillas made from fresh masa prepared by extrusion and nixtamalization processes. J Food Sci 67:1196–1199

12. **Østergård K, Björck I, Vainionpää J** (1989) Effects of extrusion cooking on starch and dietary fiber in barley. Food Chem 34:215–227

13. **Medel P, Salado S, Blas JC, Mateos G** (1999) Processed cereals in diets for early-weaned piglets. Anim Food Sci Technol. 82:145–156

14. **Vasanthan T, Gaososng J, Yeung J, Li J** (2002) Dietary fiber profile of barley flour as affected by extrusion cooking. Food Chem 77:35–40

15. **Milán-Carrillo J, Gutiérrez-Dorado R, Cuevas-Rodríguez E O, Garzón-Tiznado JA y Reyes-Moreno C** (2004) Nixtamalized flour from quality protein maize (Zea mays L). Optimization of alkaline processing. Plant Foods Hum Nutr 59:35–44

16. **AACC** (2001) Approved Methods of American Association of Cereal Chemist. 10th ed. National Academic Press, Washington, D.C.

17. **AOAC** (1995) Official Methods of Analysis, 16th ed. Association of Official Analytical Chemists, Washington, D.C.

18. Norma Oficial Mexicana-062-ZOO-1999 (1999) Especificaciones técnicas para la producción, cuidado y uso de los animales de laboratorio. Secretaría de Agricultura, Ganadería, Desarrollo Rural, Pesca y Alimentación, Estados Unidos Mexicanos.

19. **Gutiérrez-Dorado R, Ayala-Rodríguez AE, Milán-Carrillo J, López-Cervantes J, Garzón-Tiznado JA, López-Valenzuela, JA, Paredes-López, O. Reyes-Moreno, C** (2008) Technological and nutritional properties of flours and tortillas from nixtamalized and extruded quality protein maize (*Zea mays* L.). Cereal Chem 85:808–816

20. **Dahlin K, Lorenz K** (1993) Protein digestibility of extruded cereal grains. Food Chem 48:13–18

21. **Soetan KO, Oyewole OE** (2009) The need for adequate processing to reduce the antinutritional factors in plants used as human foods and animal feeds: A review. Afr J Food Sci 3:223–232

22. **Bornet F** (1993) Technological treatments of cereals. Repercussions on the physiological properties of starch. Carbohyd Polym 21:195–203

23. **Ranhotra GS, Gelroth JA, Astrote K, Eisenbraun GJ** (1991) Effect of resistant starch on intestinal responses in rats. Cereal Chem 68:130–132

24. **Perales J, Gutiérrez R, Milán J. Bello L, Reyes C** (2005) Cambios en el almidón de maíz de calidad proteínica durante la producción de harinas instantáneas y tortillas. Rev Ciencia y Tec 3:150–154

25. Food and Agriculture Organization of the United Nations (1993) Physical and chemical changes in maize during processing. In Maize in human nutrition. FAO Series 25. Rome

26. **Wisker E, Bach K, Daniel M, Feldheim W, Eggum B** (1996) Digestibilities of energy, protein, fat and nonstarch polysaccharides in a low fiber diet and diets containing coarse or fine whole meal rye are comparable in rats and humans. J Nutr 126: 481–488

27. Food and Agriculture Organization of the United Nations (1998) Physiological effects of dietary fibre. In: Carbohydrates in Human Nutrition. FAO Food and Nutrition Paper–66. Rome

28. **Kahlon TS, Chow FI, Hoefer JL, Betschart AA** (2001) Effect of wheat bran fiber and bran particle size on fat and fiber digestibility and gastrointestinal tract measurements in the rat. Cereal Chem 78:481–484

29. **Cummings JH, Hill MJ, Jenkins DJ, Pearson JR, Wiggins HS** (1976) Changes in fecal composition and colonic function due to cereal fiber. Amer J Clin Nutr 29:1468–1473

30. **Munakata A, Iwane S, Todate M, Nakaji S, Sugaguara K** (1995) Effects of dietary fiber on gastrointestinal transit time, fecal properties and fat absorption in rats. Tohoku J Exp Med 176:227–238

31. **Mälkki Y, and Virtanen E** (2001) Gastrointestinal effects of oat bran and oat gum. A review. Lebensm.-Wiss. U.-Technol. 34:337–347

International Biotechnology Color Journal

A Hitchhiker's Guide to the Modeling of the Three-Dimensional Structure of Proteins

Eneas Chavelas-Adame[1,2], Eric E. Hernández-Domínguez[1], Samantha Gaytán-Mondrangón[1], Luis Rosales-León[1,3], Lilián Valencia-Turcotte[1] and Rogelio Rodríguez-Sotres[1,*]

[1] Departamento de Bioquímica, Universidad Nacional Autónoma de México.

[2] present address: Universidad Autónoma de Guerrero. Av. Javier Méndez Aponte No. 1, Fracc. Servidor Agrario, Chilpancingo, C.P. 39070, Gerrero, México.

[3] Present address: Facultad Medicina, UNAM.

**To whom all correspondance should be sent.*

Chief Editor: José J. Zúñiga-Aguilar. Area Editor: Susana Lozano. Recieved: April 8, 2011. Revised version: June 4, 2011. Accepted: July 31, 2011.

Abstract

The functionality of a protein is strongly dependent on its spacial conformation, but the experimental methods to determine its three-dimensional structure are time-consuming and their success is no guaranteed. While only 20 amino acids are present in the amino acid sequences of most proteins, the full exploration of the many amino acid sequence combinations and their many possible spacial conformations is out of reach, even for the most powerful computer systems currently available. However, given a known amino acid sequence, with unknown 3D-structure, some strategies have been devised to propose a feasible structural model. Then, the main limitation is to produce a quality score of the 3D-model, that bears some relationship with natural structure. Here we review some highly successful methods for the generation of protein structural 3D-models by homology modeling, and present the use of some of the available quality scores, including the novel Rd.HMM protocol [Martínez-Castilla L.P. & Rodríguez-Sotres R., PLoS ONE 5(2010), e12483]. This last quality score is the only one scoring the 3D-model's fitness to truly host the target amino acid sequence, as it is able to identify those natural amino acid sequences that the 3D-model represents best. Emphasis is put on non-commercial software and open-access internet services.

***Contact address:** *Departamento de Bioquímica, Facultad de Química, Universidad Nacional Autónoma de México. Ave. Universidad No 3000. Cd. Universitaria, Coyoacán, C.P. 04510, Mexico D.F. México. Phone: (+52)5556225285. Fax:(+52)5556225329. e-mail: sotres@servidor.unam.mx*

Abbreviations: *3D, three-dimensional; PDB, protein data bank; Rd, ROSETTA design, HMM, hidden Markov model; Rd.HMM ROSETTA design-HMMER scoring protocol.*

Keywords: *Protein three-dimensional structure, protein structure homology modeling, protein structure quality score, protein structure appropriateness. Protein structure reverse folding. Hidden Markov model.*

Gold: *Bioinformatics*

Introduction

The three-dimensional structure of proteins can be experimentally determined mainly through X-ray crystallography, neutron diffraction, and multidimensional NMR. All of these techniques have their limitations and success is not guaranteed in any of them. One of the main limitations is the time needed to resolve the complete structure. In contrast, modern sequencing techniques have yielded a huge number of amino acid sequences for many different natural proteins. As an example, in january 2011, the UniProt/Swiss-Prot included 524420 distinct protein sequences (1), but the PDB (2) contained 40 thousand entries with a difference of at least 1 amino acid. That is to say, only for 7.8 % of the proteins with known amino acid sequence the 3D-structure is also known. In consequence, methods to predict the conformation of a protein from its amino acid sequence, with certainty, would be extremely valuable (3). However, the number of possible conformations of a polypeptide chain is too large to be explored, even by nature, so proteins must reach their native 3D structure through specific paths (4)- While we ignore the keys to the protein folding pathways, clearly they are rather complex (5). Several approaches to the problem have been devised, which can render a 3D-model of a protein structure starting form its amino acid sequence, and then the main limitation lies in the quality assessment of such model. Available methods can be grouped in ab initio and comparative modeling (6). However these models can be inadequate at two different levels. At the global level, the model is correct if the folding pattern reflects what we would find in nature; at the local level, the model is correct if the angles, distances and contacts are consistent with the chemical and physicochemical properties of proteins. Then the task becomes, as the Eisenberg's group pointed out, "to distinguish between a mistraced or wrongly folded model, and one that is basically correct, but not adequately refined" (7). In theory, the grounds to answer this question is in the energy difference between the unfolded and the folded protein, however, this energy difference may be as small as a few hydrogen bonds, salt bridges, and/or van der Walls contacts (8). In addition, the energy of a native protein structure is quite variable and does not correlate with its size, compactness, or the number of non-local contacts (9). A proper calculation of the molecular energy requires the use of quantum chemical calculations, but approximations to the calculation of this energy for macromolecular systems have only very recently been available, and still are computationally very demanding (10). Instead, approximations, designated as molecular mechanics, have been developed using classical mechanical forces (or force-fields), that try to reproduce the structural and physicochemical properties of molecular systems (11) Many molecular mechanics force-fields are available, yet, these energy calculations carry an intrinsic systematic error. According to calculations published by Faver et al. (12), the local systematic error in the calculations propagate to the entire protein and their magnitude soon becomes larger than the energy difference between the native and other misfolded, or partially folded states. Therefore, a low calculated energy may be informative, but can not be the only criterion to establish a 3D-model's adequacy, and most important, the energy magnitude tells very little about its resemblance with the folding adopted by the protein of interest, in its natural environment.

The present paper attempts to compare some non-commercial and successful methods to the homology modeling of the protein 3D structure, and to provide some basic guidelines to the analysis of the quality and appropriateness of the resulting model. It does emphasize the value of the recently published protocol Rd.HMM (13) as a tool to rate the model appropriateness, since this is the only tool available that renders a quantitative measure of this essential piece of information.

Materials and Methods

Three amino acid protein sequences were modeled using several strategies, including the SWISS MODEL repository (14, 15), I-TASSER (16, 17), Pro-sp3-TASSER (18, 19), SAM-T08 server (20, 21), the 3D-JIGSAW server (22, 23), and the Pcons meta server (24, 25), which gathers several methods, but their predictions were considered at the 3 and 11 methods stages, without the inclusion of SAM-T08. At the 3 methods stage, the Pcons meta server gives the best model obtained from PCONS PMODELLER, PconsM blast , and hhpred2 rpsblast. At the 11 method stage, the Pcons meta-server also includes lfugue, lhhsearch15, lppa-i, lprospect2, lsp3, lsparks2, muster, and nfold rpsblast.

In addition, other models for the same sequences were built using MODELLER (26, 27), a hidden Markov-based multiple alignment guided by the HHpred/HHmod server (28, 29).

SWISS-MODEL is considered and old method, and, as will be shown below, its models may be defective, however, it is still used by some authors to produce models and derive conclusions reported in high impact journals (30,31). 3D-JIGSAW is also somehow old, but again, it is still in use (32). In this last case, the X-ray crystallographic structure of the Saccharomyces cereviciae isomaltase (PDB codes 3AJ7, 3A47 and 3A4A) was solved a few months after the paper was published, and confirmed the validity of the 3D-JIGSAW prediction.

The refinement of some of the obtained structures was done using HyperchemTM, with the AMBER99 force field in the vacuum, using a slow convergence procedure than has been described elsewhere (33). This protocol was applied to models with severe structural defects, which can be identified by visual inspection using VMD (34). Other tool to improve the models was the ROSETTA relax-fast protocol (35). ROSETTA relax-fast improves many structural features of the model, including the packing of the side chains and proteins compactness, however, this method may fail to solve some defects, such as long peptide bonds, because these defects are treated as chain breaks. ROSETTA relax-fast may also fail to relax regions were packing is too tight. Since

Hyperchem is a commercial program, a license is needed to use it. An alternative is MODELLER (26, 27), which has an academic license, that can be obtained at no cost (26). In order to perform the minimization, the "optimize.py" script (http://salilab.org/modeller/examples/scoring/optimize.py) needs to be run. In the script the path pointing to the local folder need to be changed (change the line starting with env.io.atom_files_directory), as well as the file name (change the line starting with "code"). It is also possible to modify the parameters to increase the minimization stringency. An example of its effectiveness is given below for target 3.

The different models either raw or after refinement were then compared in their ability to produce geometrically and energetically acceptable models, using the ANOLEA (36) energy, and the GROMOS energy (37), as implemented in the "swiss PDB viewer" software (38), and were scored for their biologically appropriateness using Rd.HMM (13). The sequence database employed for the Rd.HMM was a small sequence database including the target sequences, and some unrelated amino acid sequences picked up at random form the NCBI Refseq database (39), but only the scores obtained against the sequence intended to model are presented, for reasons of brevity. The Rd.HMM result is a list of the amino acid sequences in the scanned database fulfilling a cut-off criterion (the default is E-value equal or below 10). The cut-off limits here were relaxed to allow the target sequence to be included in every test, despite its score and E-value. Frequently, in homology modeling and threading, the resulting model's 3D coordinates recover the template's amino acid sequence on top of the target sequence, with better score and lower E-value. A good model should score the target amino acid sequence on top of any other natural sequence, including the template. For X-ray solved structures, the ratio of the Rd.HMM score to the length of the model's amino acid sequence should be about 0.6 (13), but ROSETTA-relaxed (35) 3D models give a ratio slightly above 1 (33).

In this work, the resulting Rd.HMM score is presented as percentage of the length of the sequence covered by the 3D-structural model under analysis. The Rd.HMM score is the decimal logarithm of a ratio of two probabilities, i.e. the probability of the observed sequence to fit into the model divided by the probability of the observed sequence to appear in a set of random sequences (null hypothesis). The better the model, the larger the quotient, and the score will be large and positive. Negative values are a sign of a very poor coincidence between the backbone coordinates of the proposed 3D-model and its putative amino acid sequence. It is perfectly possible for a model to give a low energy score, but a negative Rd.HMM score. In this case, the model may represent a local energy minimum, but it is unlikely to be the native one, that is to say, it is not biologically appropriate. According to our previous report (13) a value close to 60% is to be expected for structures determined experimentally by X-ray diffraction. Relaxation of the 3D-models with the ROSETTA relax fast (35) may result in scores close to 100% (33), or higher. The E-values, scaled to a 10 million sequences database, are given as the negative of its decimal logarithm. The larger this last value, the smaller the probability of a accidental meaningless match; values of 1.30 or below (including negative values) lack of statistical significance (p level 0.05). Taken together, low Rd.HMM scores, with no statistical significance for a given target sequence, are indicative of a 3D-model with backbone 3D-atomic coordinates unfit to host the target amino acid sequence. Since that amino acid sequence is the one intended to model, low Rd.HMM scores and -Log(E-value) indicate a biologically inappropriate model, which could indicate either a wrong template or an inadequately refined model (7). When severe structural defects have been corrected, specially if the last step uses ROSETTA relax-fast, a low Rd.HMM score indicates a wrong model. Unlike other quality assessment methods for protein 3D-models Rd.HMM does not give false positives (13). Instead false negatives may occur frequently and a model with low Rd.HMM score is not yet appropriate, but in some cases it may be improved to become so. In other words, discarding a model as a starting point should not be done based on the Rd.HMM score only.

An additional criterion of quality should be the length of the amino acid sequence covered by the model. Currently, of the methods included here, when the available templates do not cover the whole target sequence, only the SAM-T08, I-TASSER and Pro-sp3-TASSER will attempt to include the unaligned part in the model. The HHpred/HHmod protocol can be forced to include the unaligned part, but this part is modeled usually with a very poor guess. The Pcons metaserver is a site that combines many of the strategies used by other servers, including some of the ones used here. The models in Pcons are then scored according to their own quality predictor. Pcons models were taken at the 3 methods and, if different from these last model, at the 11 methods stages also. These stages include the HHpred/HHmod strategy, but no the SAM-T08 methods. The Pcons server allows you to resubmit the unaligned sequence, but this option was not tested here. In the HHpred server some user intervention is required, and templates are chosen either automatically or manually. In our case, the templates were chosen using the automatic selections strategy and then models were prepared using the well established software MODELLER (26, 27).

These servers were chosen considering their response times, and their robustness, and in some cases, their use in the literature. Servers such as Robetta (40), Meta-TASSER (41) and Raptor (42) are suitable choices, all producing very robust models. Some of these programs, such as I-TASSER, ROSETTA (Used by the Robetta server) and Meta-TASSER, can be downloaded. Raptor can be acquired as a commercial program, but it was not evaluated here.

To get an idea of how easy was the task given to the servers the target sequences were aligned using the NCBI-blast service (39), against the sequences in the PDB.

Results

The three-dimensional structure for three proteins was modeled using several strategies. These amino acid sequences were chosen because of they are not so large, so calculation times can be cut down, because their 3D-structure is unknown, and because they are annotated to posses activity, either as an enzyme (target 3) or as an electron carrier of an enzyme (targets 1 and 2). These three sequences are presented in figure 1, and their putative active site residues, as annotated at the NCBI site (39) from classical bioinformatic considerations, are underlined.

The sequences depicted in figure 1 were submitted to several servers for automatic 3D-structure prediction and each model was scored as described in the methods section, either as produced

Target 1. Pyruvate formate-lyase activating enzyme from *Desulfovibrio vulgaris* str. Hildenborough. REFSEQ accession NC_002937.3. Residues 1 to 297.

```
  1 MRQGMIYNIQ RMSVHDGPGL RTTVFLKGCP LRCLWCSNPE SQSAVPQMLF FENLCTGCGK
 61 CVEVCPEGAA RIVDGKVIRS IAKCTHCGLC TASCPSKARE MSGRLMTVEE VMDVVLKDML
121 FYENSGGGVT FGGGEPTSGG EFFLDLVKAA HEEGIHVTVD TCGFCPEERF DRTLALADLF
181 LFDCKHTDPE AHRRLTGQDN TLILRNLRAA LASGKEVHVR MPLIPGMNDD DANLSALAAL
241 LGEFGRDKVE VMPCHAFGWN KYVALGLPAP DMPQYTPEQL SAVLDRFAKH GLVPVMV
```

Target 2. NADH dehydrogenase ubiquinone, subunit I, from *Xenopus (Silurana) tropicalis*. REFSEQ accession: NM_001006929.2. Residues 1 to 209

```
  1 MLVVRLIQNA VKRPGVSCTQ MLSRPLSLAS QMHSYKYVNA REEATDLKSV TDRAAQTLLW
 61 TELFRGLGMT LSYLFREPAT INYPFEKGPL SPRFRGEHAL RRYPSGEERC IACKLCEAVC
121 PAQAITIEAE PRTDGSRRTT RYDIDMTKCI YCGFCQEACP VDAIVEGPNF EFSTETHEEL
181 LYNKEKLLNN GDKWEVEIGA NIQADFLYR
```

Target 3. L-3-hydroxyacyl-Coenzyme A dehydrogenase, from *Strongylocentrotus purpuratus*. REFSEQ: accession XM_782095.2. Residues 1 to 292

```
  1 MAAIKNVTIV GGGQMGAGIA QVAAQTGHAV TVVDLSQQVL DNSMAYIQKS LARIAKKKYA
 61 EDPAGGTEFV NSILGSISMV TDAESAVGSS DLVIEAIIEN IKIKQDLFSK LDKVAPANTI
121 FVSNTSSLQI SDIASVTSRK DRFGGLHFFN PVSMMKLVEV VRINDTSEET YNSLMDFSKA
181 LGKTPITCRD TPGFVVNRLL VPYMCEAVRM IERGDATTRD VDIGMKLGAG YPMGPFELVD
241 YVGVDVIKFI LDGWHESYPD EALFQPSETI NKLVADGKLG VKTGEGFYKY NK
```

Figure 1. Amino acid sequences of the tree targets selected for this paper. A) Target 1: Putative pyruvate formate-lyase activating enzyme from Desulfovibrio vulgaris str. Hildenborough. (NCBI-RefSeq accession YP_011484). The conserved active site motif is underlined (aa 87 to 94). B)Target: Putative subunit of the NADH dehydrogenase complex (ubiquinone Fe-S oxidorreductase) from Xenopus (Silurana) tropicalis. (NCBI-RefSeq accession NP_001006930). The putative 4Fe-S4 binding motifs are underlined C) Target 3: Putative L-3-hydroxyacyl-Coenzyme A dehydrogenase, (short chain specific) from Strongylocentrotus purpuratus (RefSeq accession: XP_787188). The Putative NAD+ binding domain is underlined.

by the server or after minimization (33) and/or relaxation (35). The ANOLEA (36) and GROMOSS (37; 38) energies, and the score and -log(E-value) from the Rd.HMM protocol (13) are shown in tables 1 to 3, for targets 1 to 3, respectively. The Rd.HMM protocol can produce a list of related sequences, yet the scores shown here are only those for to the corresponding target. In a good protein structural model the target sequence should come at the top or nearly at the top of such list and must score better than the template used to produce the model. Poor or wrong models may give empty lists, since Rd.HMM has been found to produce no false negatives, if positive Rd.HMM scores and E-values below one are used as cut-off limits (13).

Target 1.

The first sequence belongs to a sulphur bacteria and is annotated as a pyruvate formate-lyase activating enzyme. The enzymes of this family family handle free radicals, thanks to a iron-sulfur cluster and S-adenosylmethionine in close proximity. They active site presents a conserved 4Fe-4S binding motif (Fig 1A, double underline).

Table 1 shows the scores and energies for the models obtained for this protein. The closest relatives in the PDB were 3C8F_A and 3CB8_A with only 20% identities and 42% homology (after introduction of 24% gaps) and covered 95% of the target sequence. The models provided by Pcons and

Table 1. Quality scores for various three-dimensional models of the amino acid sequence for target 1 (NCBI-RefSeq accession: YP_011484;). Putative pyruvate formate-lyase activating enzyme form *Desulfovibrio vulgaris* str. Hildenborough.

Model origin	Refinement	Sequence coverage	Rd.HMM		ANOLEA energy	GROMOS forcefield
		Start ... End [a]	Score [b] (%)	-Log (E-value) [c]	E/kT units (Zscore)	kJ/mol
Swiss-Model	none	3 ... 296	16.6	0.7	+4195(13.3)	$+1.69\times10^{7}$
Swiss-Model	ROSETTA-FR [d]	3 ... 296	65.9	51	-1779(1.17)	[h] $+1.7\times10^{7}$
HHpred/HHmod	none	1 ... 297	12.6	-2.8	+813(6.68)	+6599.1
HHpred/HHmod	ROSETTA-FR	1 ... 297	83.5	67.3	-1679(1.5)	[h] +5121.4
SAM-T08	none	31 ... 72 [f]	-59	-7.3	+273(13.5)	$+7.08\times10^{7}$
SAM-T08	AMBER99 [e]	1 ... 297	37.9	25.5	-2475(0.44)	-4898.7
SAM-T08	ROSETTA-FR	1 ... 297	91.3	74.3	-1712(1.57)	-6676.9
SAM-T08	AMBER99 &ROSETTA-FR	1 ... 297	94.2	76.9	-1947(1.17)	-6224.8
Pcons 3 methods [g]	none	2 ... 292	14.4	5.3	-35(4.88)	7.25×10^{12}
Pcons 3 methods	ROSETTA-FR	2 ... 292	77.7	60.7	-1589(1.15)	-4840.4
I-TASSER, mdl 3	none	88 ... 293 [f]	-124	-1	-471(4.30)	-101.4
I-TASSER, mdl 3	ROSETTA-FR	1 ... 297	83.5	67.4	-1630(2.07)	-5727.9
psTASSER,mdl 3	none	1 ... 297	-18.3	2.4	+3454(11.9)	3.98×10^{10}
psTASSER,mdl 3	ROSETTA-FR	1 ... 297	60.8	54.1	-1689(1.96)	[h] $+1.63\times10^{9}$
psTASSER, mdl3	AMBER99	1 ... 209	13.5	4.77	-1985(2.15)	-1152.4
psTASSER, mdl3	AMBER99 &ROSETTA-FR	1 ... 209	82.6	66.5	-1403(3.46)	-4676.8

Notes: [a] Sequence full length was 297 aminoacids.
[b] As percentage of the length of the sequence covered by the model
[c] Scaled to a 10 million sequences database, values above 1.30 indicate statistical significance.
[d] ROSETTA 2.31 fast-relax protocol.
[e] Hyperchem TM slow minimization on AMBER 99.
[f] Reduced coverage derives from the inability of the Rd.HMM protocol to score the whole sequence, due to geometrical defects in the modeled structure, or to nomenclature problems in the PDB file structure.
[g] Pcons after 11 methods still considered the 3 methods prediction as best
[h] Unusually high energy is mainly due to only a few extremely strained bonds, and/or a few atom clashes.

SWISS MODEL lacked a few amino acids at the beginning. 3D-JIGSAW gave no model for this sequence, and the other models covered the full sequence. With the exception of the I-TASSER model, the starting raw models were of poor quality, because the ANOLEA and GROMOS energies are high and the Rd.HMM scores are low, with little on none statistical significance (Table 1). I-TASSER and Pro-sp3-TASSER (psTASSER) produced several models, but only the one given the best Rd.HMM score after relaxation is presented. The SAM-T08 model was structurally defective, due to very long peptide bonds at some specific positions. When defects in the SAM-T08 model were corrected with slow minimization under AMBER99, its score improved and gained statistical significance. Further relaxation with ROSETTA relax-fast gave the best model for this target, yet, this 3D-model still has room for improvement, since its Rd.HMM score is below 100%, which is the expected value for ROSETTA-relaxed structures. The SAM-T08 after minimization and relaxation is considered best because its Rd.HMM score is higher, its ANOLEA and GROMOS energies were both negative and large, and because it includes the full 297 amino acids. The cartoon representation of this model is presented in figure 2A, where the active site conserved motif CxxxCxxC is show as balls and sticks. The orientation was chosen to make evident the deep cavity of the putative active site. The average distance between the sulphur atoms of C29, C33 and C36 is 5.63 Å roughly 0.5Å below the average Cys-Cys distance in the 4Fe-4S binding motif observed in PDB structure 3CF8.

Comparison between all the ROSETTA relaxed models (Fig. 2B) and the final model (Fig 2B, cartoons) illustrates the high sensitivity of Rd.HMM, because the overall fold at the protein core looks very similar, yet the score does show important variations, and improves dramatically after minimization and/or relaxation of the structures. The molecular mechanics slow minimization protocol eliminated the serious structural defects of the starting structures for the SAM-T08 (Fig 2C) and for the pro-sp3-TASSER (Fig. 2D) models. The Cα rmsd of the SAM-T08 models, taking the best model as reference was 2.00 Å for the starting raw model, 1.53 Å for the AMBER minimized model and 2.25 Å for the ROSETTA fast-relaxed model. The I-TASSER model was a better starting model, but after the correction

Table 2. Quality scores for various three-dimensional models of the amino acid sequence of target 2. (NCBI-RefSeq accession NP_001006930;). Putative subunit of the NADH dehydrogenase complex (ubiquinone Fe-S oxidorreductase) from *Xenopus (Silurana) tropicalis*.

Model origin	Refinement	Sequence coverage	Rd.HMM		ANOLEA energy	GROMOS forcefield
		Start ... End [a]	Score [b] (%)	-Log (E-value) [c]	E/kT units (Zscore)	kJ/mol
3D-JIGSAW	none	66 ... 209	-32.6	-6.6	+314(7.22)	3941.6
3D-JIGSAW	ROSETTA-FR [d]	69 ... 209 [f]	54.3	16.07	-427(2.49)	-1048.9
Swiss-Model	none	3 ... 209	-5.2	-3.08	-268(3.21)	-3398.9
Swiss-Model	ROSETTA-FR	3 ... 209	47.7	10.82	-585(1.35)	-4123.9
HHpred/HHmod	none	3 ... 209	-58.4	-7	+3375(15.9)	5990.7
HHpred/HHmod	ROSETTA-FR	1 ... 209	38.9	17.4	148(5.61)	-2644.6
SAM-T08	none	31 ... 72 [g]	-18.2	-6.81	670(8.12)	[h] $+1.34\times10^{7}$
SAM-T08	AMBER99 [e]	1 ... 209	44.5	21.2	-744(1.95)	-5577.6
SAM-T08	ROSETTA-FR	1 ... 209	3.9	-1	-508(2.68)	-5778
SAM-T08	AMBER99 & ROSETTA-FR	1 ... 209	61.5	31.7	-779(1.94)	-6218.4
Pcons 3 methods	none	86 ... 173	-18.8	-4.5	-125(3.78)	[h] $+1.02\times10^{5}$
Pcons 3 methods	ROSETTA-FR	83 ... 173	19.5	-1.18	-482(1.13)	-1236.2
Pcons 11 methods	none	83 ... 209	-3.1	-3.43	+110(5.63)	[h] $+1.15\times10^{6}$
Pcons 11 methods	ROSETTA-FR	83 ... 209	22.3	12.3	-533(2.02)	-2857.3
I-TASSER, mdl2	none	1 ... 209	0.1	6.2	-364(3.58)	-1710.3
I-TASSER, mdl2	ROSETTA-FR	1 ... 209	47	29	-789(1.90)	-6280.3
psTASSER, mdl2	none	7 ... 208 [f]	-32.9	0.8	+1676(11.7)	[h] $+1.55\times10^{10}$
psTASSER, mdl2	ROSETTA-FR	1 ... 207 [f]	37.1	23.1	-508(2.78)	[h] $+1.03\times10^{4}$
psTASSER, mdl2	AMBER99	1 ... 209	3	-0.15	-1056(0.64)	-4528.4
psTASSER, mdl2	AMBER99 & ROSETTA-FR	1 ... 209	77.6	41.8	-609(2.31)	-5503.3

Notes: [a] Sequence full length was 209 aminoacids.
[b] As percentage of the length of the sequence covered by the model
[c] Scaled to a 10 million sequences database, values above 1.30 indicate statistical significance.
[d] ROSETTA 2.31 fast-relax protocol.
[e] Hyperchem™ slow minimization on AMBER 99.
[f] Reduced coverage derives from the inability of the Rd.HMM protocol to score the whole sequence, due to geometrical defects in the modeled structure, or to nomenclature problems in the PDB file structure.
[g] Reduced coverage is due to the Rd.HMM protocol to score the whole sequence, due to geometrical defects in the modeled structure, or to nomenclature problems in the PDB file structure.
[h] Unusually high energy is mainly due to only a few extremely strained bonds, and/or a few atom clashes.

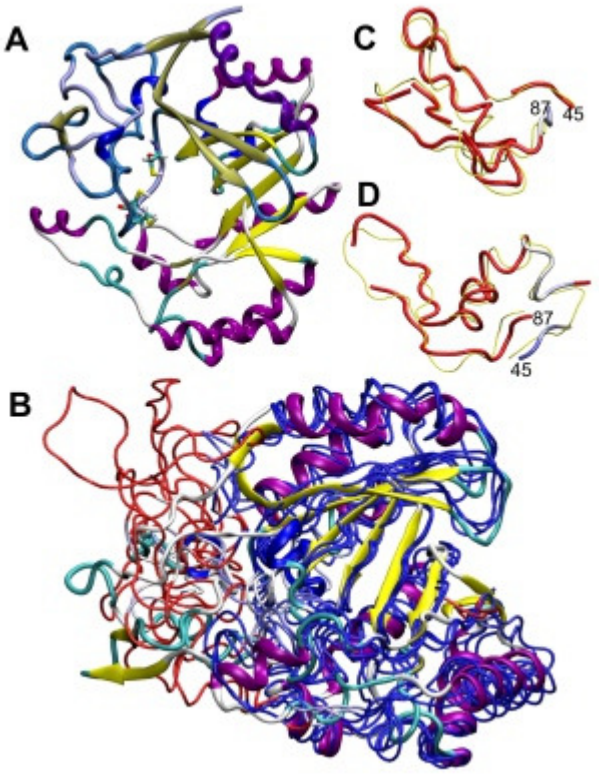

Figure 2. A) Best model for target 1 from SAM-T08 server after minimization with molecular mechanics and ROSETTA relax-fast as cartoons. The region with a bluish shadow is the N-terminal domain. The active site cysteine residues 29, 33 and 36 are shown as licorice. B) Structurally superimposed tube representation of the models relaxed with ROSETTA relax-fast, from all the servers included in table 1. The model shown as cartoons is the same as in A. Regions in blue indicate a structure and sequence match. Red regions are divergent predictions. C) Tube representation of the regions formed by amino acids 45 to 86 as predicted by the SAM-T08 server, before (red) and after (yellow) molecular mechanics refinement (see table 1). D) Tube representation of the regions formed by amino acids 45 to 86 as predicted by the Pro-s3p-TASSER server, before (red) and after (yellow) molecular mechanics refinement (see table 1). Images were prepared with VMD (34).

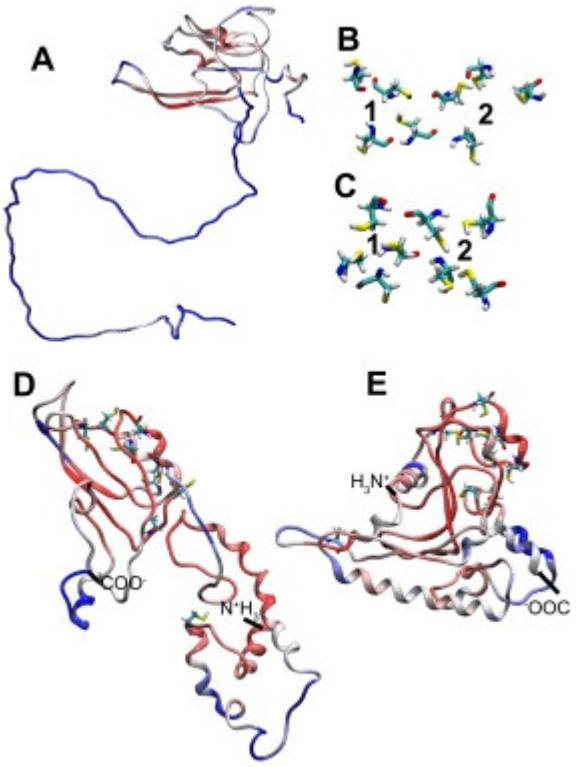

Figure 3. Predicted models for the target 2 amino acid sequence (see table 2). A) Cartoon representation of the HHpred/HHmod 3D-model after relaxation with ROSETTA fast-relax. B) Licorice representation of the putative cysteine binding sites for the two (numbered) 4Fe-4S active site clusters of the Pro-sp3-TASSER minimized and relaxed 3D-model. C) Licorice representation of the putative cysteine binding sites for the two (numbered) 4Fe-4S active site clusters of the SAM-T08 minimized and relaxed 3D-model. D) Cartoon representation of the Pro-sp3-TASSER minimized and relaxed prediction. E) Cartoon representation of the SAM-T08 minimized and relaxed prediction. In A, D and E cartoons are colored according to combination of local ANOLEA an GROMOS energies per residue. Blue unfavorable high energy values, neutral intermediate energy values, red favorable low energy values. Images were prepared with VMD (34).

of structural defects and ROSETTA relaxation the SAM-T08 was better. The pro-sp3-TASSER model after relaxation reached a negative ANOLEA energy, a positive Rd.HMM and statistical significance, yet the GROMOS energy was still very high, reflecting the presence of structural defects that ROSETTA fast-relax was unable to correct. The defects in this last model were eliminated again after slow minimization with Hyperchem (table 1). After relaxation the Pro-sp3-TASSER model was as good as the I-TASSER model and close to the SAM-T08 model.

Target 2.

This sequence belongs to the one subunit of the NADH dehydrogenase from a frog and possesses two sequences identified as possible 4Fe-4S binding motifs (Fig. 1, double underline). The protein is part of a large membrane-bound enzyme, but this subunit is in the soluble fragment. The closest relative in the PDB is 2FUG, subunit 9, which shares 46% identity and 61% homology with only 5% gaps, but covers only 60% of the whole sequence. Therefore 2FUG:9 is a good template for only part of the sequence.

Again, table 2 shows the models recovered from several servers and their quality scores. All the servers were able to produce a model, with the SAM-T08, the I-TASSER, the pro-sp3-TASSER, and the HHpred/HHmod covering the whole sequence. All the raw models were poor, as judging from the very low Rd.HMM scores and -Log(E-values), as well as, in many cases, the large positive ANOLEA and GROMOS energies (Table 2, refinement none). After relaxation, all models improved significantly, because their Rd.HMM scores were now positive, their -Log(E-value) indicated statistical significance and, except for the HHpred/HHmod and the Pro-sp3-TASSER cases, the ANOLEA and GROMOS energies were negative. The Pro-sp3-TASSER and the SAM-T08 required minimization and relaxation and then became the best models, yet, in both cases, the Rd.HMM score was well below the target value of 100%. Figure 3A shows the HHpred/HHmod relaxed model where the N-terminal segment is unfolded, due to the lack of alignment to any of the templates, and figures 3B and 3C show a close up of the iron-sulfur binding cysteines for the Pro-sp3-TASSER and the SAM-T08

models, respectively. There are two putative 4Fe-4S binding sites located on the C-terminal domain (see Fig. 3D and 3E) with similar geometries in both predictions, but the SAM-T08 prediction has a slightly more compact and better geometry to accommodate the Fe-S clusters. The Cα rmsd of the SAM-T08 models, taking the best model as reference were 3.23 Å for the starting raw model, 2.42 Å for the AMBER minimized model, and 3.86 Å for the ROSETTA fast-relaxed model. Again the I-TASSER was a better starting model, but after refining, the SAM-T08 was a bit better. In addition, the GROMOS energy of the Pro -sp3-TASSER model was high, as with the target 1 Pro-sp3-TASSER model. In this case, after minimization with Hyperchem and relaxation with ROSETTA, the Pro-sp3-TASSER model had a better Rd.HMM score, yet, it was still below the target score of over 100%, and its ANOLEA and GROMOS energies are higher than the ones for the SAM-T08 model. Figure 3D shows the Pro-sp3-TASSER minimized and relaxed model, and Figure 3E shows the SAM-T08 model also after minimization and relaxation. In both predictions, the protein shows two domains, and though the models' amino and carboxy-terminal domains belong to the same folding class in both models, the two predictions are clearly rather different. The coloring scale shows the regions with unfavorable energy in blue. Those regions tend to cluster on the surface of the predicted 3D-models. The core regions are reddish indicating favorable energies.

Target 3

Target 3 corresponds to a possible L-3-hydroxyacyl-Coenzyme A dehydrogenase, with short chain specificity, from the sea urchin. This sequence was 63% Identical to 3HDH and had 79% homology, without any gaps in the alignment and covering 98% of the target sequence. The classic NAD binding Rossman-fold domain comprises residues 6 to 193 and is underlined in figure 1.

The 3D-models for this sequence were of good quality, even before any refinement, as judging from the positive Rd.HMM scores, statistical significance and the negative ANOLEA energies (table 3, refinement none). Only the SAM-T08, the Pro-sp3-TASSER, and the Pcons (at 3 and 11 methods) gave positive GROMOS energies, indicative of defects in geometrical features or in residue-residue contacts. After refinement with ROSETTA relax-fast, all models, except the Pro-sp3-TASSER one, gave Rd.HMM scores

Table 3. Rd.HMM scores for various three-dimensional models of the amino acid sequence for target 3 (NCBI-RefSeq accession: XP_787188;). Putative L-3-hydroxyacyl-Coenzyme A dehydrogenase, (short chain specific) from *Strongylocentrotus purpuratus*.

Model origin	Refinement	Sequence coverage	Rd.HMM		ANOLEA energy	GROMOS forcefield
		Start ... End [a]	Score [b] (%)	-Log (E-value) [c]	E/kT units (Zscore)	kJ/mol
Swiss-Model	none	4 ... 290	24.1	6.9	-1644(0.52)	-8244.5
Swiss-Model	ROSETTA-FR [d]	4 ... 290	106	84.6	-2153(-0.39)	-9812.6
HHpred/HHmod	none	1 ... 292	53.2	39.9	-1407(1.24)	-730.8
HHpred/HHmod	ROSETTA-FR	1 ... 292	110	89.3	-2263(-0.49)	-6730.1
SAM-T08	none	1 ... 289 [f]	-28.3	8.6	-1246(1.97)	7253.2
SAM-T08	AMBER99 [e]	1 ... 292	52.4	39.1	-2526(-0.79)	-6142.8
SAM-T08	ROSETTA-FR	1 ... 292	109	88.1	-2273(-0.44)	-9512.5
SAM-T08	AMBER99 & ROSETTA-FR	1 ... 292	114	93.3	-1949(0.34)	-6590.3
Pcons 3 methods	none	4 ... 290	40.3	27.5	-1382(1.27)	406.7
Pcons 3 methods	ROSETTA-FR	4 ... 290	115	92.2	-2326(-0.64)	-6795.2
Pcons 11 methods	none	4 ... 290	30	18.9	-1014(2.13)	[h] $+4.15\times10^{6}$
Pcons 11 methods	ROSETTA-FR	4 ... 290	101	79.8	-2029(-0.10)	-6375.4
I-TASSER, mdl 1	none	4 ... 292 [f]	37.7	12.9	-1168(1.34)	-1137.8
I-TASSER, mdl 1	ROSETTA-FR	1 ... 292	111.4	97.6	-1897(1.04)	-7019.9
psTASSER, mdl 2	none	1 ... 292	-56.2	8.11	1912(4.72)	[h] $+1.32\times10^{7}$
psTASSER, mdl 2	ROSETTA-FR	1 ... 292	80.3	70.3	-1608(1.60)	[h] $+4.58\times10^{9}$
psTASSER, mdl 2	AMBER99	1 ... 292	22.1	12.1	-2376(-0.11)	-4716.4
psTASSER, mdl 2	AMBER99 & ROSETTA-FR	1 ... 292	97	77.9	-2167(0.16)	-6184.8
psTASSER, mdl 2	MODELLER	1 ... 292	-11	-3.41	-529(2.2)	5670.7
psTASSER, mdl 2	MODELLER & ROSETTA-FR	1 ... 292	92.6	74.1	-1965(0.41)	-4177.7

Notes: [a] Sequence full length was 292 aminoacids.
[b] As percentage of the length of the sequence covered by the model
[c] Scaled to a 10 million sequences database, values above 1.30 indicate statistical significance.
[d] ROSETTA 2.31 fast-relax protocol.
[e] Hyperchem™ slow minimization on AMBER 99.
[f] Reduced coverage is due to the introductions of gaps in the Rd.HMM alignment at the start or end of the query sequence.
[g] Reduced coverage is due to the Rd.HMM protocol to score the whole sequence, due to geometrical defects in the modeled structure, or to nomenclature problems in the PDB file structure.
[h] Unusually high energy is mainly due to only a few extremely strained bonds, and/or a few atom clashes.

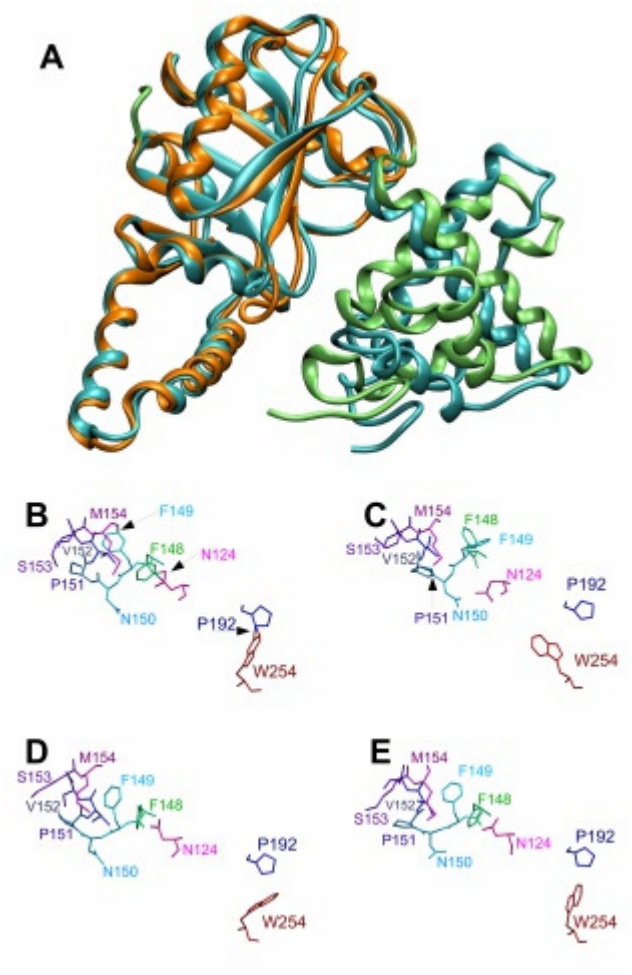

Figure 4. Predicted models for the target 3 amino acid sequence (see table 3). A) Superposition of the SAM-T08 (minimized and relaxed, cyan cartoons) and the Pcons (3 methods, relaxed, orange or green cartoons) models for target 3 (see table 3). The orange region represents the putative NAD+ binding domain (underlined in figure 1C). B) to E) show the detailed licorice view of residues 124, 148 to 154, 192 and 254 for the Pro-sp3-TASSER model 2 prediction. B) As provided by the server. C) After refinement with ROSETTA-fast-relax. D) After minimization with Hyperchem E) after minimization with MODELLER. Arrows point to spots where atom clashes were detected, and such defects can be identified by the aberrant atom bonding patterns. Images were prepared with VMD (34).

over 100%, indicative of good, well refined structures, with the characteristic ROSETTA fast-relax bias (33), and with large negative energies for both ANOLEA and GROMOS potentials. In this case, the Pcons 3 methods, relaxed, and the SAM-T08 minimized and relaxed 3D-models were the best, closely followed by the I-TASSER and the swiss model predictions, but again, the Pcons presents a few missing residues at the termini, while the SAM-T08 model includes the whole target sequence. Figure 4A shows a superposition for the Pcons 3 methods, relaxed model (Fig 4A, orange and green cartoon) and the SAM-T08 minimized and relaxed model (Fig 4A cyan cartoon). The putative dehydrogenase NAD+ binding domain is shown in orange for the Pcons model, and both models had only 1.21 Å Cα rmsd, in this N-terminal domain. The C-terminal domain presents larger differences with a Cα rmsd of 6.05 Å, but still the overall fold is similar.

The Cα rmsd of the SAM-T08 models, taking the best model as reference was 1.31 Å for the starting raw model, 1.22 Å for the AMBER minimized model, and 2.96 Å for the ROSETTA fast-relaxed model. The results with the I-TASSER and Pro-sp3-TASSER models followed the same trend as with targets 1 and 2, and after refinement, both were close to the SAM-T08 model, though not better.

In addition, with this target, the Pro-sp3-TASSER model was minimized using MODELLER (with the internal CHARMM force-field; 27). This minimization was less effective than the Hyperchem protocol, as judged from the quality indexes. However, MODELLER can be obtained at no cost with an academic license, and consumes considerably less computer resources. If the model is intended to be used in Molecular Dynamics simulations, the simulations imply further refinement, and then the MODELLER minimization may be enough to ready the model for the simulation run. Figures 4B to 4E show a close up to residues 124, 148 to 154, 192 and 254, for the Pro-sp3-TASSER model 2, as provided by the server (Fig. 4B), after ROSETTA relax-fast refinement (Fig. 4C), after minimization with MODELLER (Fig. 4D), and after minimization with Hyperchem (Fig. 4E). The starting model form the server had several atom clashes, shown here by the wrong connectivity indicated by the arrows (Fig 4B). ROSETTA fast-relax was able to correct some of the problems, but at the expense of a new atom clash in P151 (Fig. 4C). Instead classical minimization protocols with molecular mechanics were able to eliminate the atom clashes and produce acceptable geometries. As mentioned previously, ROSETTA fast-relax also did fail to correct long peptide bonds. Therefore, ROSETTA fast relax is a good protocol only is the starting geometry is not too distorted, otherwise, a minimization step using classical molecular mechanics should precede the ROSETTA relax-fast refinement.

With this last target, the minimized and ROSETTA fast-relaxed SAM-T08 model was better only when the Rd-HMM, the ANOLEA and the GROMOS energies are taken together, because, if only the ANOLEA energy is considered, the AMBER99 minimized model was better, and if only the GROMOS energy is considered, the ROSETTA fast-relaxed model was better.

Discussion

In two out of the three cases, the SAM-T08 models were poor at the beginning, but turned out to be better after refinement (minimization and relaxation). Apparently, the SAM-T08 server tends to give essentially well folded models, but unrefined. The other servers tested can give better starting geometries, particularly the I-TASSER models, but in the end the models were not better than the SAM-T08 model. It is to be noted that I-TASSER models are numbered according to the server score, but not

necessarily model 1 was better when analyzed with Rd.HMM. The Pro-sp3-TASSER models were improved by the ROSETTA fast-relax, but their GROMOS energies were still positive. This was indicative of structural defects susceptible of correction with an approach similar to the one taken for the SAM-T08 models. In one case (target 2), the resulting refined model was equivalent in quality to the SAM-T08 model, but since the two predictions have important differences in their folding patterns, and because both are below the optimal level of Rd.HMM score, both may be considered as possible starting points to seek for a better model. From this last piece of evidence, a warning arises, as no single server will render the best model on all cases, and predictions should be obtained from more than one server. The final goal is a model with a Rd.HMM score of 60% before relaxation (ROSETTA fast-relax), above 100% after ROSETTA fast-relaxation, and with good structural quality scores (as low ANOLEA and GROMOS energies, for instance).

Models produced with templates with less than 40% homology to the template are known to have low quality. However, in our set, the worst model was the one for target_2, which presented a homology of almost 60% to at least 1 template. Therefore, one must not assume that a high homology to a template is enough to guarantee a good final 3D-model. The length of the sequence covered by one single template, as well as the percentage of gaps required to produce an alignment are also very important criteria. Here, target 2 is the sequence with the shorter sequence covered by a single template in the initial NCBI-blast search. Instead, the 3D-models for target 3 gave the best results and this sequence presented high homology, almost full coverage, and no gaps in the alignment to one single template in the initial blast. Clearly, at such high level of template and target sequence homology, all servers do an acceptable job.

Conclusion

The use of Rd.HMM scores, together with additional quality measures such as ANOLEA and GROMOS energies allows the identification of 3D-models with a biologically relevant folding pattern and well refined. One useful procedure for refinement is the ROSETTA fast.-relax protocol, but this must be combined with a molecular mechanics minimization step to correct some structural defects that ROSETTA fast-relax does not eliminate. In general terms, the chances of a successful modeling job may be assessed using a simple Blast of the target sequence to the sequences in the PDB database. However, sequence homology does not suffice to indicate the usefulness of a template. The length of the target sequence covered by the template and the number of gaps required to produce a good alignment must also be considered.

In general terms, SAM-T08 seems to be a good choice because it gives results fast and produces better folded models, even for targets with no obvious templates. However, the SAM-T08 3D-models are poorly refined and should be minimized with classical molecular mechanics, and perhaps relaxed with ROSETTA fast-relax to produce a well refined model. The Pro-sp3-TASSER can also produce good, but poorly refined models. The I-TASSER server produces well refined initial models, but after refinement and relaxation, other servers can produce models just as good, or even better. With these last two servers, the model rated as best by the server is not necessarily the best after refinement. Clearly, no single server can be trusted to produce the best models in all cases, and even when some possible templates are detected, there is no guarantee for success.

Assessment of the model is essential, and a quality index indicative of a biologically appropriate 3D-model is the Rd.HMM score, and its corresponding E-value, however, other tools must be used to detect poorly refined models.

Acknowledgments

This work was financially supported by CONACyT (México) CB-2008-01-0101186, PAPIIT-DGAPA UNAM IN210909, PAIP-FQ-UNAM, and the Super-computing facilities at DGSCA-UNAM.

References

1. **Uniprot Consortium** (2010) The Universal Protein Resource (UniProt) in 2010. Nucleic Acids Res 38:D142–148
2. **Rose P W , Beran B, Bi C, Bluhm W F, Dimitropoulos D, Goodsell DS, Prlic A, Quesada M, Quinn GB, Westbrook JD, Young J, Yukich B, Zardecki C, Berman HM, Bourne P E** (2011) The RCSB Protein Data Bank: redesigned web site and web services. Nucleic Acids Res 39:D392–401
3. **Sali A, Kuriyan J** (1999) Challenges at the frontiers of structural biology. Trends Cell Biol 9:M20–42
4. **Levinthal C** (1968) Are there pathways for protein folding? J Chim Phys 65:44–45
5. **Dinner AR, Sali A, Smith LJ, Dobson CM, Karplus M** (2000) Understanding protein folding via free-energy surfaces from theory and experiment. Trends Biochem Sci 25:331–339
6. **Xiang Z** (2006) Advances in homology protein structure modeling. Curr Protein Pept Sci 7:217–227.
7. **Luthy R, Bowie JU, & Eisenberg D** (1992) Assessment of protein models with three-dimensional profiles. Nature 356:83–85
8. **Mixcoha-Hernández E, Moreno-Vargas L, Rojo-Domínguez A, Benítez-Cardoza C** (2007) Thermal-unfolding Reaction of Triosephosphate Isomerase from *Trypanosoma cruzi*. Protein J 26:491–498
9. **Melo F, Feytmans E** (1998) Assessing protein structures with a non-local atomic interaction energy. J Mol Biol 277:1141-1152
10. **He X, Merz KM** (2010) Divide and Conquer Hartree-

Fock Calculations on Proteins Journal of Chemical Theory and Computation 6(2):405–411

11. **Hu Z, Jiang J** (2010) Assessment of biomolecular force fields for molecular dynamics simulations in a protein crystal. J Comput Chem 31:371–380
12. **Faver JC, Benson ML, He X, Roberts BP, Wang B, Marshall MS, Sherrill CD, Merz KM Jr.** (2011) The energy computation paradox and Ab Initio protein folding. PLoS ONE 6:e18868
13. **Martínez-Castilla LP, Rodríguez-Sotres R** (2010) A score of the ability of a three-dimensional protein model to retrieve its own sequence as a quantitative measure of its quality and appropriateness. PLoS ONE 5:e12483
14. SWISS-MODEL, http://swissmodel.expasy.org/, accessed on february 2, 2011
15. **Kiefer F, Arnold K, Künzli M, Bordoli L, Schwede T** (2009) The SWISS-MODEL Repository and associated resources Nucleic Acids Res 37:D387–392
16. **Zhang Y** (2008) I-TASSER server for protein 3D structure prediction. BMC Bioinformatics 9:40
17. http://zhanglab.ccmb.med.umich.edu/I-TASSER/, accessed on june 2011
18. **Zhou H, Skolnick J** (2009) Protein Structure Prediction By Pro-Sp3-Tasser. Biophys J 96: 2119–2127
19. http://cssb.biology.gatech.edu/skolnick/webservice/pro-sp3-TASSER/index.html, accessed on june 2011
20. http://compbio.soe.ucsc.edu/SAM_T08/T08-query.html, accessed in January 2010
21. **Karplus K, Karchin R, Draper J, Casper J, Mandel-Gutfreund Y, Diekhans M, & Hughey R** (2003) Combining local-structure, fold-recognition, and new fold methods for protein structure prediction. Proteins 53 Suppl 6:491–496
22. 3D-JIGSAW Protein Comparative Modelling Server, http://bmm.cancerresearchuk.org/~3djigsaw/, accessed on february 2, 2011
23. **Contreras-Moreira B, Bates PA** (2002) Domain fishing: a first step in protein comparative modelling. Bioinformatics 18(8):1141–1142
24. http://www.pcons.net/, accessed on january 10, 2011
25. **Larsson P, Skwark MJ, Wallner B, Elofsson A** (2011) Improved predictions by Pcons.net using multiple templates. Bioinformatics 27:426-427
26. http://salilab.org/modeller/, acessed on frebruary 2011
27. **Eswar N, Eramian D, Webb B, Shen M, Sali A** (2008). Protein structure modeling with MODELLER Methods Mol Biol 426:145-159
28. http://toolkit.tuebingen.mpg.de/hhpred, accessed on january 10, 2011
29. **Söding J , Biegert A, Lupas AN** (2005) The HHpred interactive server for protein homology detection and structure prediction. Nucleic Acids Res 33:W244–248
30. **Hosie AM, Wilkins ME, da Silva HMA, Smart TG** (2006) Endogenous Neurosteroids Regulate Gabaa Receptors Through Two Discrete Transmembrane Sites. Nature 444:486–489
31. **Bourdon A, Minai L, Serre V, Jais J, Sarzi E, Aubert S, Chrétien D, de Lonlay P, Paquis-Flucklinger V, Arakawa H, Nakamura Y, Munnich A, & Rötig A** (2007) Mutation Of Rrm2B, Encoding P53-Controlled Ribonucleotide Reductase (P53R2), Causes Severe Mitochondrial Dna Depletion. Nat Genet 39:776–780
32. **Brindis F, Rodríguez R, Bye R, González-Andrade M, Mata R** (2011) (Z)-3-butylidenephthalide from Ligusticum porteri, an α-glucosidase inhibitor. J Nat Prod 74:314–320
33. **Rosales-León L, Hernández-Domínguez EE, Samantha Gaytán-Mondragón S, Rodríguez-Sotres R** (2011) Metal binding sites in plant soluble inorganic pyrophosphatases. An example of the use of ROSETTA design and hidden Markov models to guide the homology modeling of proteins. J Mex Chem Soc, in press.
34. **Humphrey W , Dalke A , & Schulten K** (1996) VMD: visual molecular dynamics. J Mol Graph 14:33–8, 27–8.
35. **Raman S, Vernon R, Thompson J, Tyka M, Sadreyev R, Pei J, Kim D, Kellogg E, Dimaio F, Lange O, Kinch L, Sheffler W, Kim B, Das R, Grishin NV**, Baker D (2009) Structure prediction for CASP8 with all-atom refinement using ROSETTA. Proteins 77 Suppl 9:89–99
36. **Melo F, Devos D, Depiereux E, Feytmans E** (1997) ANOLEA: a www server to assess protein structures. Proc Int Conf Intell Syst Mol Biol 5:187–190
37. **Oostenbrink C, Villa A, Mark AE, Van Gunsteren WF** (2004) A biomolecular force field based on the free enthalpy of hydration and solvation: The GROMOS force-field parameter sets 53A5 and 53A6. J Comp Chem 25:1656–1676
38. **Kaplan W, Littlejohn TG** (2001) Swiss-PDB Viewer (Deep View). Brief Bioinform 2(2):195-197
39. **Sayers EW, Barrett T, Benson DA, Bolton E, Bryant SH, Canese K, Chetvernin V, Church DM, Dicuccio M, Federhen S, Feolo M, Geer LY, Helmberg W , Kapustin Y , Landsman D, Lipman DJ, Lu Z, Madden TL, Madej T, Maglott DR, Marchler-Bauer A, Miller V, Mizrachi I, Ostell J, Panchenko A, Pruitt KD, Schuler GD, Sequeira E, Sherry ST, Shumway M, Sirotkin K, Slotta D, Souvorov A, Starchenko G, Tatusova TA, Wagner L, Wang Y, Wilbur WJ, Yaschenko E, Ye J** (2010) Database resources of the National Center for Biotechnology Information. Nucleic Acids Res 38:D5–16
40. **Kim DE, Chivian D, Baker D** (2004) Protein structure prediction and analysis using the Robetta server. Nucleic Acids Res 32:W526–531
41. **Zhou H, Pandit S B, Skolnick J** (2009) Performance of the Pro-sp3-TASSER server in CASP8. Proteins 77 Suppl 9:123–127
42. **Xu J, Jiao F, Yu L** (2008) Protein structure prediction using threading Methods. Mol Biol 413:91–121

Recent BOOKS

Healthcare Biotechnology

A Practical Guide

Dimitris Dogramatzis, R.Ph., Ph.D.

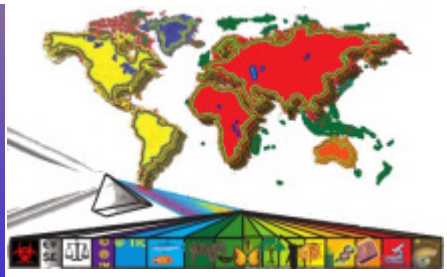

CRC Press
Taylor & Francis Group

Contact: Maikala del Castillo
CRC Press/Taylor & Francis Group

Maikala.delCastillo@taylorandfrancis.com

BRING BIOTECHNOLOGY PRODUCTS FROM THE BENCH TO BEDSIDE
With From the Trenches Guidance Every Step of the Way

Boca Raton, Florida, USA, February 7, 2011 – CRC Press announces the recent publication of **Healthcare Biotechnology: A Practical Guide** (January 2011; $99.95; ISBN 978-1-4398-4746-6) by Dimitris Dogramatzis. CRC Press functions as the principal science and technology book division of the Taylor & Francis Group, an Informa Company.

Foreseeing and planning for all of the possibilities and pitfalls involved in bringing a biotechnology innovation from inception to widespread therapeutic use takes strong managerial skills and a solid grounding in biopharmaceutical research and development procedures. Unfortunately there has been a dearth of resources for this aspect of the field. Until now. Written by a seasoned senior executive with an academic and business background, **Healthcare Biotechnology: A Practical Guide** brings a biotechnology focus and from-the-trenches style to discussions of high level concepts such as intellectual property, patent application, and commercialization, funding and partnering, R&D, biomanufacturing, "fast-track" approvals, and clinical trial design and regulations.

Focusing on the management of healthcare-related biotech, from conception through the product's regulatory approval and entire life cycle, the book provides a practical, applicable resource to assist all health-care related biotech professionals in their day-to-day activities from the lab to the boardroom. It offers more than 40 figures, 220 tables, and 180 references as well as a list of abbreviations and a business plan outline. Each chapter contains 10 questions to reinforce the material covered and 10 exercises to challenge readers and inspire critical thinking. Ancillary materials including solutions manual and over 1000 PowerPoint slides available for qualifying course adoption.

The book highlights the factors involved in determining production platforms, costs, strategies, and timelines as well as promotion, pricing, supply chain management, and bio-brand lifecycle management. A non-theoretical guide, it doesn't cover, for example, the double helix, genes, and cloning. Rather, it is a practical, day-to-day, educational resource designed to remain open on lab benches and conference room tables alike.

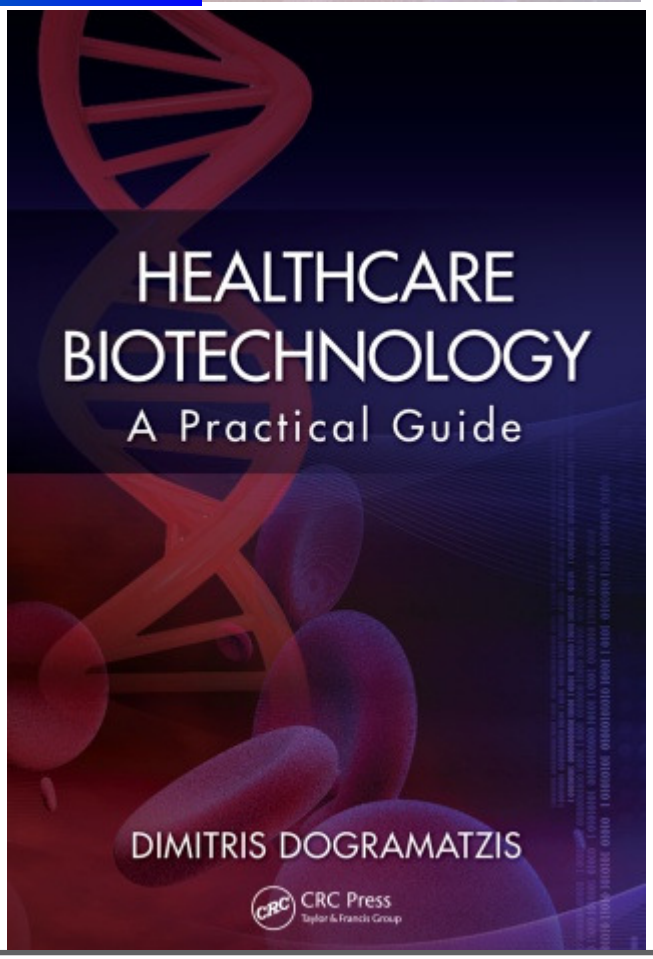

THE AUTHOR

Dr. Dimitris Dogramatzis was born in Greece in 1962. Having received a Bachelor's diploma in Pharmacy from the **University of Patras**, Greece, he spent the next seven years at Texas studying and working for the University of Texas System. During this period, he completed his Ph.D. in Pharmacology & Toxicology at the **University of Texas Medical Branch at Galveston**. Later he went on to complete two successive postdoctoral trainings at the University of Texas Medical Branch at Galveston, as well as the **M.D. Anderson Cancer Center at Houston**, Texas.
Following his return to his native Greece in 1991, he served a mandatory military service as an Army Pharmacist with the Greek Army Medical Corps, and after his discharge he joined the pharmaceutical industry. His successful industry career includes field sales, medical affairs marketing, product management, disease management, country management and regional management positions, with Hoffmann-La Roche, Lundbeck, and Serono. He has previously served as the Regional Vice President – Northern Europe for the Serono International Group, responsible for the U.K., Republic of Ireland, the Netherlands, Sweden, Denmark, Norway, Finland and Iceland markets. He is currently the owner of a retail pharmacy in Athens, a business consultant, and a writer. His professional profile can be found at: www.linkedin.com.
He has written extensively in both English and Greek, for either basic research or business publications. His academic publications include congress abstracts, full papers, and review articles, while his business publications include several interviews, full articles, two book chapters, and two books entitled "*Pharmaceutical Marketing: A Practical Guide*" (CRC Press, October 2001, ISBN-13: 978-1574911183) and "*Healthcare Biotechnology: A Practical Guide*" (CRC Press, December 2010, ISBN-13: 978-1439847466), respectively. He is a licensed skydiver and a single-engine airplane pilot. He is married and a father of two sons.

Number 1 Issue 1 October 2011

full text provided by www.ibcj.org.mx

International Biotechnology Color Journal

A Scientific Peer Reviewed Journal with Focus on BIOTECHNOLOGY and Covering Its Many Hues, Tints, Tones & Shades

MISSION

The **International Biotechnology Color Journal** (*IBCJ*) is the official trimonthly scientific Journal of the International Foundation for Biotechnology Research & Early Stimulation in the Culture of Health, Nutrition, Sport, Art, Science, Technology & Society A.C., a nonprofit corporation.

IBCJ is devoted to facilitating the advancement of our understanding of Biotechnology in its broader definition: The application of science and technology to living organisms, as well as parts and models thereof, to alter living and non-living materials for the production of knowledge, goods and services.

IBCJ is committed to publishing original contributions of research in all areas related to the theory and practice of biotechnology in its broadest context (organized by color), including research articles and notes, critical reviews, essays, book reviews, letters, correspondence, and news features or views.

IBCJ intends to provide an excellent resource for the publication of peer-reviewed research papers with proven or likely implications for the past, current, and future practice of biotechnology.

AUTHOR GUIDELINES

IBCJ will include current trends in scientific publication for the electronic format and international requirements for indexing. All manuscript should have a corresponding author. The corresponding authors assumes full responsibility for the published data, on behave of all authors.

Authors must transfer the copyright of their article for International Foundation for Biotechnology Research & Early Stimulation in the Culture of Health, Nutrition, Sport, Art, Science, Technology & Society A.C.

For review, manuscripts should be submitted to the *IBCJ* Chief editor, by e-mail, at:

"Dr. José Juan Zúñiga Aguilar" <*zuniga@cicy.mx*>

Manuscripts submitted to the *IBCJ* will be assigned to one the scientific *IBCJ* Editor, according to the section suggested by the corresponding author. The *IBCJ* Scientific editor will determine if the manuscript is within the journal scope, has high scientific quality, is presented in a manner suitable for publication in a scientific peer-reviewed journal, the content has not been published elsewhere, and if it has not been previously rejected by this journal. If the submission is considered to meet all of the above criteria, it will be forwarded to additional to referees with enough expertise in the field, for further review. Referee's names will not be disclosed, but their comments will be forwarded to the authors.

Authors should suggest the section in which their work is best placed form:

Area colors and their scope

RED	Medical Biotechnology:	*human health & disease, novel medical diagnostics and tissue engineering.*
YELLOW	Nutritional Biotechnology:	*Food, nutrition science and neutraceuticals.*
BLUE	Marine and Fresh Water Biotechnology:	*Aquaculture and fisheries; coasts and sea; fish and aquatic animals: health, nutrition, reproduction, cloning and genetic modifications, pests and disease control*
DARK GREEN	Agricultural Biotechnology:	*Biotechnology for the cultivation, processing, and storage of plants. Plant tissue culture and micropropagation. Biofertilizers, agrobiochemicals, and plant pests and disease control. Biotechnology in plant ecology and biodiversity;*
SOFT GREEN	Animal Biotechnology:	Biotechnology for the production, processing, and storage of livestock. Pets and farm-animals disease, health, nutrition, reproduction, cloning, and genetic modification.
LIME GREEN	Biotechnology of Renewable Resources:	*Bioremediation & environmental Biotechnology. Biofuels and renewable bioenergy sources, and bioenergy sources. Biotechnology and sustainable development, competitive production, biomaterials.*
BROWN	Desert Biotechnology:	*Arid zone & desert Biotechnology; space and Geomicrobiology.*
DARK	Bioterrorism:	*Human and animal pathogen manipulation, bioterrorism, biowarfare, biocrimes, anticrop warfare*
PURPLE	Patents, IPR:	*Strategy for intellectual property protection, patents, publications, inventions*
WHITE	Biotechnology of GMO's:	Industrial Biotechnology of Genetically Modified Organism's. *Gene-based industrial applications*
GOLD	Bioinformatics:	*Computer applications to the study of biological systems. Micro and nanobiotechnology, mixed biological- electronic/electromechanical systems and biomachines (MEMS and NEMS, MST and NST).*
GREY	Fermentations and Classical Biotechnology:	*Industrial biotechnology: classical fermentation & bioprocess/bioengineering technology; engineering and technological equipment for bioproduction; output of science-intensive bioproducts*
IRIS	Multidisciplinary area:	*Biochemistry, molecular biology & biotechnology, Omics applications*
PLATINUM	Synthetic Biology	*Design and obtention of new biological components, devices, and systems. Applications of re-designed natural biological systems.*
SILVER	Biobusiness, Bioentrepreneuship & Marketing:	*Development economics, Biobusiness and marketing. Strategy for innovative economical development. Improvement of the system of the S&T and innovation activities management*
TRANSPARENT	Biotechnology, Bioethics & Society:	*Assesment of the public support to the scientific activity. Biotechnological potential and human resources*
INDIGO	Integrating science, education and manufacturing:	*Education & early childhood stimulation in the culture of health, nutrition, sport, art, science, biotechnology & society as information and telecommunication technologies TIC´S*

Authors should indicate the type of work submitted form:

- CONTRIBUTION ARTICLES. Manuscripts in this category must include the following sections: Title, Authors, Authors affiliations, Contact address, phone number and e-mail of the corresponding author, Running title (60 characters maximum), Abbreviations, Abstract, key words, Introduction, Materials and Methods, Results, Discussion, Conclusion, Acknowledgments and References.

The manuscript should present results of a complete, original and verifiable research. In regular manuscripts, text should be no more than 10 pages, including tables and figures and references. With a charge to the authors, longer papers may be accepted, if the scientific value of the paper does justify so.

- NOTE. Notes must include the sections: Title, Authors, Authors affiliations, Contact address, phone number and e-mail of the corresponding author, Running title (60 characters maximum), Abbreviations, Abstract, key words, Introduction, Materials and Methods, Results, Discussion, Conclusion and References.

Manuscripts should present relevant findings, detail a brief contribution, the results of modification or improvement of previous work, or forward a novel model. Text should not be more than 20 pages. Longer contributions of this sort will not be accepted, as they will be considered as a contribution article.

- ESSAY. This contributions must include the sections: Title, Authors, Authors affiliations, Contact address, phone number and e-mail of the corresponding author, Running title (60 characters maximum), Abbreviations, Abstract, key words, Introduction, Discussion, Conclusion and References.

Essays should present critical and/or analytical contribution. Text should not be more than 10 pages.

- BOOK REVIEW. Book reviews must focus on books recently published or in press, that contribute to some relevant aspect of Biotechnology. No sections are required, and the text should not be more than 1 page.

Book reviews must present a critical and concise view of the contents and value of a recently published book.

- LETTERS TO THE EDITOR This contributions must include the sections: Title, Authors, Authors affiliations, Contact address, phone number and e-mail of the corresponding author, Running title (60 characters maximum), Abbreviations, Abstract, key words, Introduction, Discussion, Conclusion, Acknowledgments and References.

Letters to the editor should deal with topics of high relevance and/or novelty, or those of a polemical nature in any of the color areas listed above. The should be supported by appropriate recent references, and offer a novel point of view to the issue they address. The text should not be more than 3 pages.

- CORRESPONDENCE. No sections are required, and the text should not be more than 1 page. Correspondence are brief comments to enrich or criticize a previous article published in the journal. This contributions will be accepted if the Editor considers the comment relevant and of interest to the readers of ICBJ. Personal views lacking scientific support will not be accepted.

- .NEWS AND VIEWS. No sections are required, and the text should not be more than 2 pages. News and views are short comments of very recent findings published in the ICBJ, or in some other international journal. They should be brief, insightful, and well referenced.

MANUSCRIPT SUBMISSION PROCESS

All submitted manuscripts must include:

The manuscript in electronic form as a PDF file.

A cover letter addressed to the IBCJ Chief editor and signed by the corresponding author. In this letter the corresponding should indicate the section where the submitted contribution fits best. Names and addresses of three potential referees, or the name of research scientists they wish to exclude from the review process.

For submission purposes, tables and medium-quality figures may be included in the pdf document. However, the authors should accompany their submission with separate high quality figures. This must be done at the time of submission, since reviewer's may need high quality images to verify their clarity and consistency with the text.

The IBCJ Chief editor will acknowledge manuscript receipt, along with the manuscript submission code (MSC), and the name and e-mail address of the assigned IBCJ Scientific (COLOR) editor. Further correspondence relating the submission should be addressed to the IBCJ Scientific editor indicating the MSC.

Authors should contact the IBCJ Chief editor if no acknowledgment receipt has been received after a six working days.

Authors may also address the IBCJ Chief editor in case of conflict with the IBCJ Scientific editor.

The final choice of referees will be made by the IBCJ Scientific editor. If the IBCJ Scientific editor considers essential to include a reviewer, that the author has requested to exclude, the editor will first consult the corresponding author, who may then sustain or withdraw his submission.

If accepted the author will be requested to provide the text in MS_WORD 97/2000, OPEN_OFFICE_OASIS, or RICH_TEXT_FORMAT.

Do not send MS_WORD XML (docx) format, if you have prepared your MS in this format, please convert it to the old format, or to

RTF. Make sure the content of your manuscript was not altered during the conversion.

Tables and illustrations should be sent separate as graphic files. Pictures, plots, graphics, equations and schemes are considered illustrations. DO NOT EMBED EQUATIONS IN THE TEXT.

IF REQUESTED, The author should also provide a graphic abstract, and separate figures. The graphic abstract is limited to 5 cm by 10 cm (length by width).

MANUSCRIPT PREPARATION GUIDELINES

Text guidelines

Pages should be numbered and lines should be numbered and double-spaced; use Times New Roman font, 12 points size. Sections titles must be preceded by three blank lines. Paragraphs must have a four-space indention. Page size letter (21.5 x 28 cm) with 2.5 cm margins all round. Complex tables (those with unusual features) , illustrations graphs, and other supplementary materials are to be submitted separately to the text.

Illustration guidelines: The illustrations can be figures, schemes, charts, or graphics. Illustrations should be submitted as digital documents in TIFF, .JPG, or Post Script formats, and in the actual size for final version to fit in one (1962 pixels, i.e. 3.27 inches width) or two (4098 pixels, i.e. 6.83 inches width) columns with, 600 dpi resolution. Avoid figures larger than 1 page (4800 pixels height). If essential, the figure must be split into 1 page blocks (4098x4800 pixels). Illustrations with panels or insets should be numbered using letters (A, B, C, D...). Letters should be in bold-face, placed in the upper-left corner of each panel, should not be in a separate frame, and the letter size should be chosen to avoid confusion with other information in the illustration. The legend (see below) must clearly describe the contents of each subsection in the corresponding illustration.

Legend to illustration guidelines

Number your illustrations with sequential arabic numbers (1, 2, 3...). For each illustration, start the corresponding legend with a brief informative title. Then provide all essential information to make the figure clear. When not stated in the methods section, specific experimental conditions may be provided. Do not send illustrations with figures reproduced from other publications, as they may be copyright protected. If strictly necessary, the illustrations may be accepted, only if the author provides legal evidence of the due permission from the copyright owner, to the satisfaction of the ICBJ editorial board.

Table guidelines

Tables should include a Table heading and, if necessary, footnotes. Illustrations should have captions, which should be provided separate to the text. Both, table headings and illustration captions should start with a brief descriptive title, and include a short description of the contents and those experimental or technical details that are essential to the unambiguous interpretation of the data. All scientific data should be presented according to the International Units System (SI). When the introduction of a new unit of measurement is required, the unit should be clearly defined in the manuscript, base your new definitions on the SI system, as much as possible. In the case of complex tables, with special spacing, cell splitting, rare or new symbols, or other unusual features, provide your table as an illustration (see above), and include a table heading and footnotes in the "legends to illustrations" section. Sequence alignments are considered figures.

References

The references can be journal citations, whole books, theses, book chapters, book chapters in a serial publication, entries is a manual/methods compilation, and internet page addresses. Patents may be cited for reference only and as long as the patent protection is not directly or indirectly violated, for this aim, the authors must provide legal evidence of the absence of conflict, to the satisfaction of the ICBJ board. All citations should refer to internationally accessible documents. The style must conform to the next guidelines:

Documents with declared authors or editors:

Journal articles:

Author0 I J K, Author1 I K, , Author3 I L, ... , Author9 I M, et al. (1991) Article's full title. Journal CASSI serials' abbreviation 88: 3–7. DOI/PMID: xxxxx/xxxx.yy-zz.yy

Book articles:

Author0 I J K, Author1 I J, Author3 I K, ... , Author9 I J K, et al. (1991) Title of article. In I I I Editor0, I I I Editor1, eds, Book's title, Ed 2 Vol 3. Publisher, City, pp 3–7

Whole books:

Author0 I J K, Author1 I J, , Author3 I K, ... , Author9 I J K, et al. (1991) Book's title, Ed 2 Vol 88. Publisher, City, pp 3–7

Theses:

Author I J K (1991) Title of thesis. PhD thesis. University, City

Online document:

Author A (1991) Title. Source Title, http://www.domain.class.ntw/pub/info/docs/essay.html, accessed january 1, 1991.

Patent:

Inventor0 I J K, Inventor1 I J, , Inventor3 I K, ... , Inventor9 I J K, et al., inventors. January 1, 1991. Patent's full title. Patent Application Office No. 12345

Documents without declared authors or editors:

published material:

Title of Booklet, Manual, Pamphlet, etc. (1991) Publisher (or Company), City

online material:

Document's title, http://www.domain.class.ntw/pub/info/docs/form.html, accessed january 1, 1991.

If you are citing an article that exists as an online version, include the Digital Object Identifier (DOI) or the PubMed ID (PMID) number. If the paper does not exists as a printed version and has no volume, issue and pages, use one of the next styles:

Author0 I J K, Author1 I I, , Author3 I I, ... , Author9 I I, et al. (year of publication) Article's full title. PMID: 12345678

Author0 I J K, Author1 I I, , Author3 I I, ... , Author9 I I, et al. (year of publication) Article's full title. DOI: xxxx.yy-zz.yy

In the list above, Author0 up to Author 9 (or its equivalent Inventor or Editor) are the first ten authors' last names, and I J K L M are authors initials. Compound last names and special symbols must be gives as in the original publication (i.e. Zúñiga-Aguilar J J, de Villafranca Casas M J, van Beethoven L, ...). Compound initials are accepted as long as they bear special meaning (Zhi Shu J–Ch, ...). Follow the same style for inventors granted a patent. 1991 refers to the year of publication, and January, 1 1991 refers to a full date. 88 refers to journal volume, and 3–7 refers to a page range. eds, means editors; Ed, means edition; Vol, means volume; pp, mean pages. For publication cities include in parentheses the state province and/or county when confusion may arise i.e. Paris (Tx., U.S.A.). In the case of online material, references to query results, and other non-permanent internet addresses generated "on the fly" will not be accepted.

One-word journal titles should be written in full. Multiple-word journal titles should conform to the CASSI standard (http://cassi.cas.org/).
Journal names not listed in the CASSI should be written in full.
Unpublished data (submitted articles and articles in preparation) and personal communications are not acceptable as literature citations, so they must be cited in the text within parenthesis. Include initials and last names of all authors, up to 10. For articles with more than 10 authors list the first 10 and include the et al. abbreviation.

Articles that are "in press" may be so designated in "the references section" Note: An article may be referred to as "in press" only if it has been accepted for publication; cite the journal in which the article will appear, and if available, its DOI. Many journals release the online versions of papers, ahead of print. Use the style mentioned above for online material. For personal communications, it is the corresponding author's responsibility to notify those cited, and get their consent. In case of doubt, the IBCJ board may request written evidence of this.

About IFFBRAESITCOHNSASTAS AC Non Profit.

The International Foundation for Biotechnology Research & Early Stimulation in the Culture of Health, Nutrition, Sport, Art, Science, Technology & Society A.C. was founded in 2009 as a non-profit association to promote the development of professionals of biotechnology in research, industry, services, and education, and for the diffusion of biotechnological knowledge. Organizes the Biotechnology summit and Biotechnology color meeting for education that includes activities of current interest for the professionals and students working or interested in the areas of biotechnology. It also promotes the area of research, education, industry, and technological development. The International Biotechnology Color Journal (IBCJ) is the official trimonthly Journal of the International Foundation for Biotechnology Research & Early Stimulation in the Culture of Health, Nutrition, Sport, Art, Science, Technology & Society since 2011 and is devoted to the advancement of our understanding of Biotechnology (*The application of science and technology to living organisms, as well as parts and models thereof, to alter living and non-living materials for the production of knowledge, goods and services*).

Important note

These instructions for authors will appear periodically at the end of an issue, and will be available form the Journal's website. Please consult the latest instructions published, as they may change to meet new journal's requirements.

Number 1 Issue 1 October 2011

International Biotechnology Color Journal

A Scientific Peer Reviewed Journal with Focus on BIOTECHNOLOGY and Covering Its Many Hues, Tints, Tones & Shades

The International Biotechnology Color Journal appears every 4 months in the last week of February, June and October of each year, starting in October 2011. It is a non-profitable Electronic Publication. In its initial phase it does not requires neither publication nor access fees. Its goal is the publication of Original Scientific Information, previously unpublished, and provided by the contributing authors out of its own will. It is produced and Hosted by Centro de Investigación Científica de Yucatán, A.C., Calle 43 No. 130, Colonia Chuburná de Hidalgo. Mérida Yuc., Mexico. Tel: (+52) 999 942 8330. Fax: (+52) 999 942 3900. RFC. CIC791116770. Its staff does not earn a salary for the activities associated to the production of this Journal. **WEBSITE: http://www.ibcj.org.mx/**